

POLITECNICO DI TORINO

Corso di Laurea in Ingegneria Biomedica

Tesi di Laurea Magistrale

**Habit and neural fatigue: a study  
finalised to the development of a  
BCI for Locked-In subjects based  
on Single Trial EEG**



**Relatore**

Prof.ssa Gabriella Olmo

Irene Rechichi

**Correlatore:**

Ing. Vito De Feo

---

Luglio 2019

*A Lorenzo  
per il rumore e il silenzio*

## Abstract

*Author:* Irene RECHICHI

The *Locked-In Syndrome* is a medical condition regarding awake subjects that are aware and conscious but are not able to communicate verbally and physically; they are subjected to complete paralysis of almost all voluntary skeletal muscles, except for those who regulate vertical eye movements and eye-blinking. This condition is also described as *pseudocoma* and is mainly due to ventral pontine injuries. The future aim of this research project is to develop a BCI for single trial EEG analysis, that would be able to recognize specific patterns in the electrical activity of the brain, called *movement-related cortical potentials*. Among these event-related potentials, those of great interest for this study are *readiness potentials*, that generate when volitional movements are performed. The research work was divided into two parts: the experimental data collection and subsequent data analysis; habit and perceived tiredness can be listed among the factors that affect the readiness potential. In this preparatory study, the aim was to find evidence of that. Experimental data collection took several months and involved healthy subjects of age 20 to 60 and one injured subject, in minimally conscious state. The subjects underwent completely voluntary and semivoluntary tasks. The event-related potentials were extracted by simple averaging of the trials; the epochs ended with muscular activation. The algorithm successfully proved lateralization of the readiness potentials and identification of the main differences between the voluntary and semivoluntary task. In particular, by implementing a matched filter on semivoluntary task data, it was observed that the first epochs feature higher correlation, and that the latter decreases going towards the end of the trial. This suggests that habit and perceived mental tiredness affect the characteristics of the readiness potential, bringing brain electrical activity towards a *quasi*-involuntary pattern.

# Acknowledgements

When at 19 I walked into *Politecnico* to attend my first lesson, with all my expectations and fears, I could not ever imagine the wonderful Journey awaiting. During these years I met awesome people, cried with joy and out of despair... I have learnt and grown as an Engineer and, most importantly, as a Human Being.

This Master Thesis project has been a totally new experience for me, I will cherish these moments forever. I would like to thank Professor Gabriella Olmo for giving me the possibility to take part in this project, for sharing her Experience and Passion with me and my colleagues and helping me see and find the silver lining in front of me, always.

Thanks to Vito De Feo for sharing his knowledge of Neuroscience and letting me in to the crazy and surprising world of experimental research. Thanks to the people who shared this experience with me: Danilo, for his patience and helpfulness, and my colleagues Alessandro, Chiara and Leonardo for all the chats, advice and mutual help.

I would like to thank my Family, near and far, for their constant love.

Mum, Dad: I would be nothing without you. Thanks for your enduring Love and support, thanks for giving me strength and always supporting me – even when I was insanely grumpy. You already know all. And to my brother Lorenzo, thank you: you have taught me life lessons since the day you were born. Thanks for teaching me to dance in the thunderstorm... I will always be your safe haven, no matter what.

To all my dear Friends, for always believing in me. Turns out you were right all along. Enrica, thank you for being my number one supporter from day one, for all the laughs and memories made. Michela and Chiara, my fabulous BG: the days with you were sugar-coated. Thanks for the crazy laughs and the much needed hugs. To all the other people who shared this journey with me: Alessandro, Stefano, Luca, Carlo, Fabio, Chiara and Irene. These years have gone by so fast.

Last, but not least, to my partner in crime, Alberto. Thank you for sharing everything with me since the very beginning and for always being there, even when I made it so hard to put up with me. For your love, your trust, your patience: thank you. You are the best adventure companion I could ever ask for. Thanks for sharing your dreams with me. I promise you, this is only the beginning.

*Irene*

# Contents

<b>Abstract</b>	I
<b>Acknowledgements</b>	I
<b>List of Figures</b>	V
<b>List of Tables</b>	VII
<b>Introduction</b>	1
<b>1 The Central Nervous System</b>	1
1.1 General anatomy . . . . .	1
1.2 The human brain . . . . .	5
1.3 The regulation of motor control . . . . .	7
<b>2 Disorders of Consciousness</b>	10
2.1 Persistent Vegetative State . . . . .	11
2.2 Minimally Conscious State . . . . .	11
2.3 Locked-in Syndrome . . . . .	11
<b>3 The EEG Signal</b>	12
3.1 The International 10-20 System of Electrode Placement . . . . .	12
3.2 The EEG Rhythms . . . . .	14
3.3 EEG Artefacts . . . . .	16
<b>4 Event Related Potentials</b>	18
4.1 Introduction . . . . .	18
4.2 Components . . . . .	18
4.2.1 P50 . . . . .	19
4.2.2 P300 . . . . .	19
4.2.3 Contingent Negative Variation . . . . .	20
4.3 Movement Related Cortical Potentials . . . . .	20

<b>5</b>	<b>Bereitschaftspotential</b>	22
5.1	Components	22
5.2	Influencing factors	23
5.3	Generator sources	24
5.4	Free will and Libet's experiment	25
5.5	Outcomes	27
<b>6</b>	<b>Materials</b>	28
6.1	Experimental Protocol	28
6.1.1	Stage one	28
6.1.2	Stage two	29
6.1.3	Stage three	30
6.1.4	Experimental protocol in injured subjects	30
6.2	Data anonymization	32
6.3	Hardware	33
6.3.1	EEG caps and skin preparation	33
6.3.2	Electrodes	34
6.3.3	Amplifier	34
6.3.4	Acoustic signal generator and Pushbutton Pad	36
6.4	Software	37
6.4.1	Galileo Suite	37
6.4.2	EEGLAB	38
<b>7</b>	<b>Methods</b>	40
7.1	Pre-processing	40
7.2	Spatial Filtering	43
7.2.1	Spherical Spline Integral Filter	43
7.3	Data Filtering	44
7.4	EMG onset detection	45
7.5	Epochs	46
7.5.1	Averaging Technique	47
7.6	Spectral Density Estimation	48
7.6.1	EEG trials	49
7.6.2	MRCP	49
7.7	Matched Filter	50
7.8	Data analysis	52
7.8.1	First dataset	52
7.8.2	Second and third datasets	53

<b>8</b>	<b>Results</b>	54
8.1	Pre-processing and filtering results . . . . .	54
8.2	EMG Processing results . . . . .	55
8.3	Averaging results . . . . .	57
8.4	Spectral Density Estimation results . . . . .	57
8.4.1	Bandpower estimation: EEG Data . . . . .	58
8.4.2	Bandpower estimation: MRCP Data . . . . .	59
8.5	Matched Filter results . . . . .	60
8.5.1	General outcome . . . . .	60
8.5.2	Epochs details . . . . .	64
8.6	Data interpretation . . . . .	70
8.6.1	Dataset 1: results . . . . .	70
8.6.2	Datasets 2 and 3: results . . . . .	72
<b>9</b>	<b>Future development: a Machine Learning approach</b>	73
9.1	Support Vector Machine . . . . .	73
9.2	Implementation . . . . .	74
9.3	Results . . . . .	75
	<b>Conclusions</b>	77
	<b>List of Acronyms</b>	79
	<b>Bibliography</b>	82

# List of Figures

1.1	Neuron and neuroglia . . . . .	2
1.2	Meninges . . . . .	3
1.3	Spinal cord . . . . .	4
1.4	Central Nervous System, encephalon . . . . .	5
1.5	Brain lobes . . . . .	6
1.6	Cerebral cortex: functional areas . . . . .	7
1.7	Volitional movements . . . . .	9
3.1	International 10-20 Standard . . . . .	13
3.2	New international 10-20 Standard . . . . .	13
3.3	EEG Rhythms . . . . .	15
4.1	Event-Related Potential . . . . .	19
4.2	Movement related cortical potential . . . . .	21
5.1	Bereitschaftspotential . . . . .	23
5.2	Readiness Potential scalp map . . . . .	26
5.3	Libet's clock . . . . .	26
5.4	Libet's Readiness Potential . . . . .	27
6.1	Data anonymization . . . . .	32
6.2	Standard EEG Cap . . . . .	33
6.3	Pre-wired Headcap . . . . .	34
6.4	Galileo NT . . . . .	35
6.5	OpenSesame Graphical User Interface . . . . .	36
6.6	Pushbutton Pad . . . . .	36
6.7	Scalp electrodes impedance . . . . .	37
6.8	EEGLAB GUI . . . . .	38
6.9	MRCPLAB Interface . . . . .	39
6.10	Channel data . . . . .	39
7.1	Depiction of signal and noise . . . . .	41
7.2	Bode Diagram, Butterworth 11 . . . . .	42

7.3	Bode Diagram, Butterworth, 3	42
7.4	Legendre Polynomial	45
7.5	Creating epochs	46
7.6	Motor Related Cortical Potentials, averaging technique	47
7.7	Grand Average Plot	48
7.8	Hamming window	49
7.9	Matched filter output, channel FP2	51
7.10	Matched filter output, channel FP2 (2)	51
8.1	EEG Channel Data	55
8.2	Current Source Density	55
8.3	LabJack output signal	56
8.4	Impulsive EMG and relative onset	56
8.5	Motor Related Cortical Potentials	57
8.6	Grand Average MRCP	58
8.7	Matched filter output, channel FP1	61
8.8	Matched filter output, channel FP2	61
8.9	Matched filter output, channel AF3	62
8.10	Matched filter output, channel AF4	62
8.11	Matched filter output, channel FCz	63
8.12	Matched filter output, channel FP2. Subject 5.	63
8.13	Channel FC1, epoch 1 detail	64
8.14	Channel FC1, epoch 1 detail	65
8.15	Channel FC1, epoch 13 detail	65
8.16	Channel FC1, epoch 22 detail	66
8.17	Channel FC1, epoch 33 detail	66
8.18	Channel FP1, epoch 1 detail	67
8.19	Channel FP1, epoch 7 detail	67
8.20	Channel FP1, epoch 14 detail	68
8.21	Channel FP1, epoch 25 detail	68
8.22	Channel FP1, epoch 32 detail	69
8.23	Pearson Coefficient. Mean	70
8.24	Pearson Coefficient. Standard Deviation	71
8.25	Pearson Coefficient. Skewness	71
8.26	A comparison: task 1 vs task 2	72
9.1	Support Vector Machine	74
9.2	Support Vector Machine, Training Set: scatter plot	75
9.3	SVM, Confusion Matrix	76
9.4	SVM, Receiver Operating Characteristics	76

# List of Tables

3.1	Biopotentials . . . . .	14
5.1	BP influencing factors . . . . .	25
6.1	Skin impedance . . . . .	34
8.1	Bandpower percentage results of healthy subjects channel data. . . . .	59
8.2	Bandpower estimation of Motor Related Cortical Potentials . . . . .	59
8.3	Pearson coefficient. Dataset 1, voluntary task. . . . .	70

# Introduction

*... his whole appearance produced on the mind the impression of a corpse with living eyes, and nothing could be more startling than to observe the expression of anger or joy suddenly lighting up these organs, while the rest of the rigid and marble-like features were utterly deprived of the power of participation ...*

With these words, in 1846 novel *The Count of Monte Cristo* Alexandre Dumas father described Mr Noirtier de Villefort, who after suffering an apoplectic stroke became mute and paralyzed, able to communicate only through the use of his eyes. Imagine to open your eyes, and feel what it would be like to be awake, conscious and aware of the surrounding environment but not being able to interact with it: this is the *Locked-In Syndrome* (LIS). The LIS can be described as a *supranuclear quadriplegia* combined with intact vertical eye movement functions [17]; the subjects affected by this condition show inability to speak, as they lack coordination between breathing and voice, that prevents them from producing voluntary sounds – though their vocal cords are not affected by the paralysis. Although suffering from permanent paralysis, their consciousness and awareness is preserved. It is caused by injuries limited to the area of the *pons*, that damage the efferent fibers; an exhaustive explanation on Central Nervous System anatomy is carried out in Chapter 1. It is not uncommon that patients in the locked-in state are mistakenly diagnosed as persistent vegetative state (PVS) subjects. The field of the Disorders of Consciousness is vast and between LIS and PVS there is a spectrum of indefinite conditions that go under the name of *minimally conscious state*; they will be dealt with in Chapter 2. Brain-Computer Interfaces (BCIs) expanded the frontiers of Biomedical Engineering and Neuroscience; to this purpose, a BCI could be employed in order to establish a communication pathway between the injured subjects and an external machine and to facilitate the recovery process of neural functions. In the past two decades BCIs offered encouraging outcomes if applied to healthy subjects but, as regards clinical studies, they have not been widely employed yet [13]. The aim of this preparatory study is to investigate the nature of brain electrical patterns that arise during the actualization of volitional movement and the factors that affect their occurrence; they are found under the form of *motor related cortical potentials* and will be described in detail in Chapter 4 and Chapter 5. Different signal processing

methods will be applied to prove the effect of habit on electroencephalographic activity during the execution of repetitive tasks. Furthermore, in the view of future development, the implementation of a Machine Learning algorithm made it possible to compare the brain patterns generated both in volitional movement actualization and semi-voluntary task performance, paving the way to automatic recognition of brain electrical activations.

# Chapter 1

## The Central Nervous System

The human central nervous system – also said CNS – is made of the brain and the spinal cord; it is the processing centre of the human body and contains about  $10^{11}$  neurons connected to each other by  $10^{14}$  synapses. The CNS has many purposes, in fact, it is responsible for human perceptions and feelings, voluntary decision-making and thinking. Furthermore, its main function is to maintain homeostasis, that is the tendency to resist change in order to keep a stable internal environment; by doing so, the CNS coordinates the activity of all human organs. It is very vulnerable to physical trauma and it is protected and supported by glial cells, connective tissue, cerebrospinal fluid (CSF) and bones.

### 1.1 General anatomy

As mentioned before, the CNS is a very complex structure that is capable of coordinating all human activities; it consists of the brain and spinal cord and of all the anatomical structures that provide support and protection. The two main classes of cells are neurons and glial cells. All these structures will be described in detail in the following paragraphs.

#### Neurons

Neurons are excitable cells that communicate by means of electrical impulse transmission. They are able to generate quick electrical signals of large amplitude, called *action potentials*. Neurons consist of three components (Figure 1.1):

- a compact cellular body (or *soma*) containing the nucleus, it is responsible of protein synthesis and cellular metabolism;
- *dendrites*, that branch off the nucleus and receive information from other neurons thanks to the *synapses*;

- a single *axon*, another neural fiber extruding from the soma that is in charge of sending information to multiple neurons.

Information propagates along the axons in the form of action potentials, briefly modifying the membrane potential: the inside of the cell becomes more positive with respect to the outside.

### Glial cells

Around 75-90% of the central nervous systems consists of glial cells (*neuroglia*), non-neuronal cells that provide mechanical support to neurons (Figure 1.1). There are different types of neuroglia, among which the most important are *astrocytes* and *microglia*. Microglia are phagocytes responsible of protecting the CNS from bacteria and cellular debris; they also protect neurons from oxidative stress. Astrocytes are star-shaped cells that are very differentiated and thus are able to perform several tasks in the CNS. They play an important role in the maintenance of the extracellular environment balance, especially as regards extracellular potassium levels. Moreover, they are able to eliminate neurotransmitters such as glutamate and biogenic amines, that, if present in excess, could lead to neural damage. Astrocytes regulate the development and regeneration of synapses and axons and provide biochemical support of endothelial cells forming the blood-brain barrier.

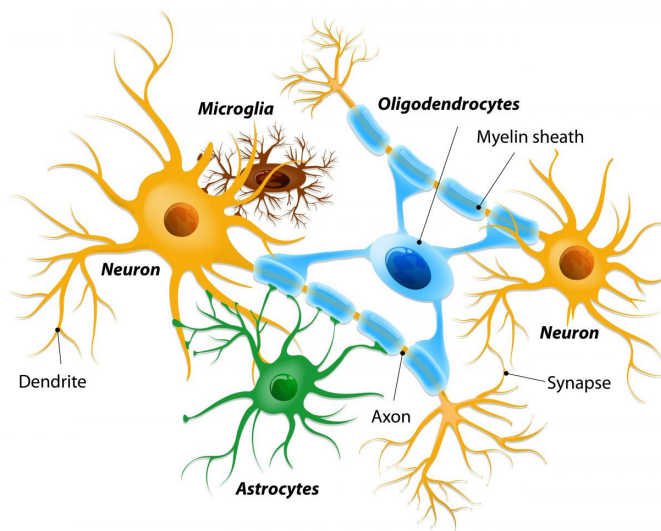


Figure 1.1: A neuron and neuroglia. It is possible to observe dendrites, axons, astrocytes, microglia and oligodendrocytes; adapted from [7]

## Meninges and cerebrospinal fluid

The outermost structures providing physical support to the CNS are the skull – protecting the brain – and the spinal column, that surrounds the spinal cord. However, these two structures may represent a mechanical risk for the CNS: in case of impact, their stiffness could damage the nervous tissue that is extremely delicate. Due to this issue, the CNS receives further protection by the *meninges* and *cerebrospinal fluid* (CSF). The meninges are three layers of connective tissue that surround the brain and spinal cord (Figure 1.2). The outermost membrane is the *dura mater*, made of tough fibrous tissue, the intermediate layer is called *arachnoid mater* – due to its shape – and the innermost membrane is the *pia mater*, characterised by a softer tissue. Between the arachnoid and pia matres is located the *subarachnoid space*, a cavity that is filled with CSF. This body liquid is found also in other cavities of the encephalon and surrounds neurons and glial cells. It provides mechanical protection to the CNS, in fact, it acts as shock absorber in case of impacts and prevents collision between the nervous systems and the hard skull; moreover, just as astrocytes, helps maintaining the correct ionic balance.

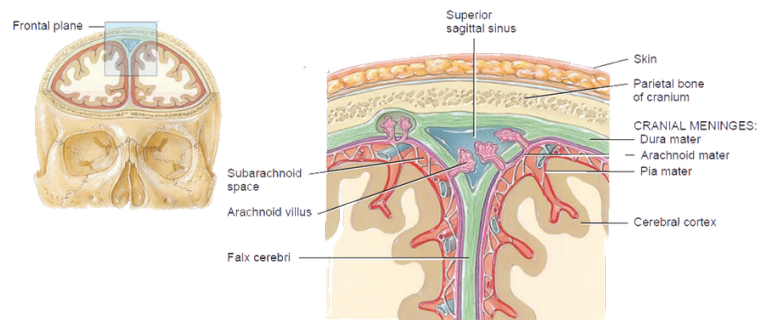


Figure 1.2: The three meninges. On the left they are seen from a frontal plane, on the right they are seen in detail. It is possible to recognise the dura mater, arachnoid and pia mater.

## Grey and white matter

The central nervous system is characterised by a very definite neural arrangement. Cellular bodies, dendrites and axon terminals form clusters that appear grey to the eye, and axons form white agglomerates. Grey matter takes about 40% of CNS and is the place where integration of information occurs. White matter occupies the remaining 60% and is responsible for quick transmission of information. The brain is covered by a layer of grey matter, called *cerebral cortex*; white matter is found below and features small clusters of grey matter underneath, called *subcortical*

*nuclei*. As regards the spinal cord, the arrangement is different: white matter lays on the outside and is supported by grey matter.

## The spinal cord

The spinal cord is a cylindrical structure made of nervous tissue that originates from the *medulla oblongata* in the brainstem and is surrounded by the spinal column. It is about 45 *cm* long and has a diameter of 1.4 *cm*; it extends from its origin to the first *lumbar vertebra*, where it ends and makes way for the *cauda equina*, a group of spinal nerves that occupies the last portion of the spinal column and consists of cervical (C1-C8), thoracic (T1-T12), lumbar (L1-L5), sacral (S1-S5) and coccygeal (C0) nerves (Figure 1.3). White matter is organized in ascending and descending tracts that connect peripheral nerves to the encephalon; the ascending pathways transmit information from the spinal cord to the brain, the descending ones pass down information from the brain to the spinal cord. It should be noted that both pathways are bilateral; however, most of them cross towards the opposite side creating contralateral fibers. Most of sensory and motor pathways are contralateral, meaning that sensorial information regarding the right-half of the body is processed in the left hemisphere and, in the same way, motor control of the right-half of the body generates in the left brain.

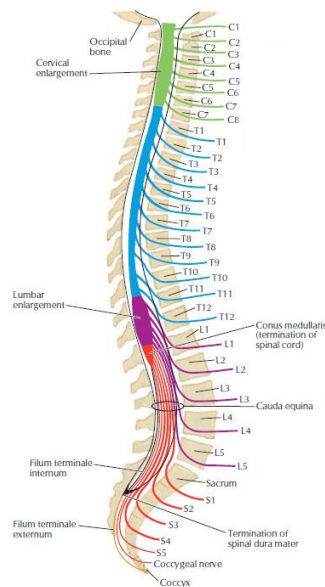


Figure 1.3: The spinal cord and its spinal nerves (C-cervical, T-thoracic, L-lumbar, S-sacral, coccygeal). The cauda equina is also shown. Adapted from [31]

## 1.2 The human brain

The encephalon consists of the forebrain, cerebellum and brain stem; the forebrain includes the brain and diencephalon. The brain, or *cerebrum*, is a C-shaped organ divided into two parts, called emispheres, by the longitudinal fissure (Figure 1.4). The cerebral emispheres are made of white matter and surrounded by a thick layer of grey matter, the cerebral cortex. White matter takes about 60% of the CNS and is responsible for quick transmission of information. The integration of information occurs in the grey matter, of which also basal ganglia are made. As regards the spinal cord, the arrangement is different: white matter lays on the outside and is supported by grey matter.

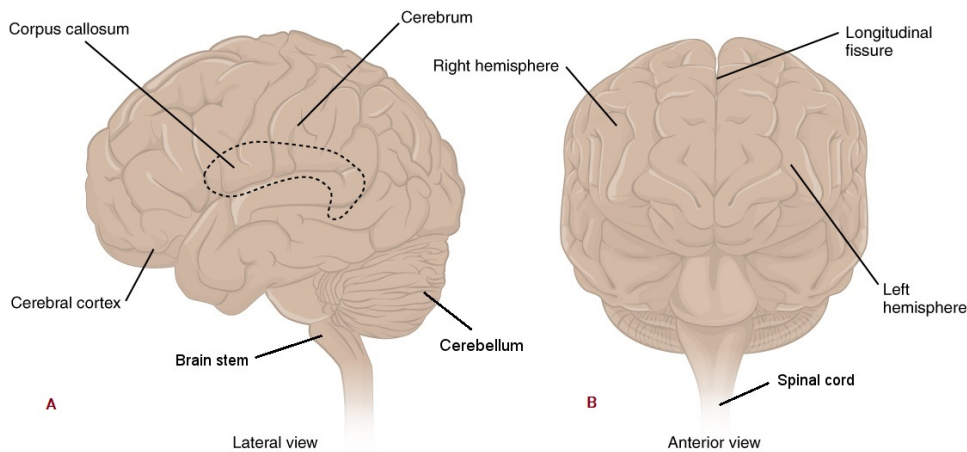


Figure 1.4: The encephalon. A) Lateral view of the encephalon, brainstem and cerebellum are shown. B) Anterior view of the encephalon: it is possible to observe the two emispheres and the longitudinal fissure. Adapted from [1]

### Diencephalon

Diencephalon is located just below the brain and consists of two medial structures: the *thalamus* and *iphotalamus*. Thalamus is an aggregation of *subcortical nuclei*; it plays a significant role in sensory processing and motor control. In fact, sensorial information in order to reach the cerebral cortex passes through the thalamus, where it is filtered and modified. The ipothalamus is found below the thalamus; it is responsible for homeostasis and ensures communication between the nervous and endocrine systems. It is mostly subjected to the control of the autonomic nervous system (ANS), for this reason, it releases hormones from the anterior and posterior *hypophysis* in response to electrical or chemical signals.

### Cerebral cortex and functional areas

As mentioned before, the cerebral cortex is the outer layer of grey matter in the cerebrum; it is responsible for the integration of sensory impulses, directing motor activity, and controlling higher intellectual functions. It is found only in mammals, and in large specimens the surface area is increased by the presence of *sulci* and *gyri* – forming a highly convoluted layer of grey matter (Figure 1.4,A). There are two major furrows: the central sulcus (or *fissure of Rolando*) and the lateral sulcus (or *Sylvius' fissure*); they divide the cortex into four areas: the occipital, temporal, parietal and frontal lobes (Figure 1.5).

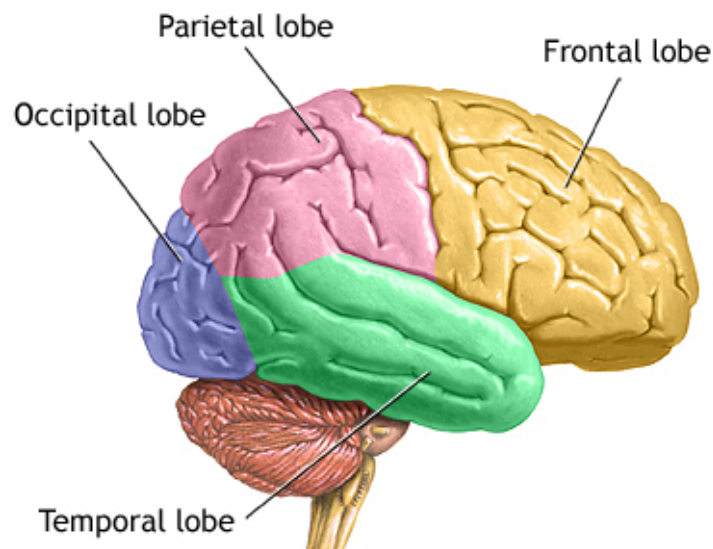


Figure 1.5: The four brain lobes: frontal, occipital, temporal, parietal; adapted from [5]

The frontal lobe, as the name suggests, is located in the fore area of the brain and is limited at its back by the fissure of Rolando, that separates it from the parietal lobe, that is found between the central sulcus and the occipital lobe. The temporal lobe is found in both hemispheres, it is located beneath frontal and parietal lobes, and is separated from the former by the lateral sulcus. Inside each lobe, the cerebral cortex has a very specific functional organization (Figure 1.6). The occipital lobe is responsible for the processing of visual information – in fact, it is also indicated as *visual cortex*; the temporal lobe regulates the auditory processes (*auditory cortex*) but it is also responsible for learning and language control. The parietal lobe's main functions regard the integration of *somatic* sensory information and proprioception. The frontal lobe is responsible for personality, language and motor control: in fact, it consists of the primary motor cortex (PMC), that is involved in the generation

of volitional movements and performance of attention-requiring tasks, pre-frontal cortex, pre-motor cortex and supplementary motor area (SMA).

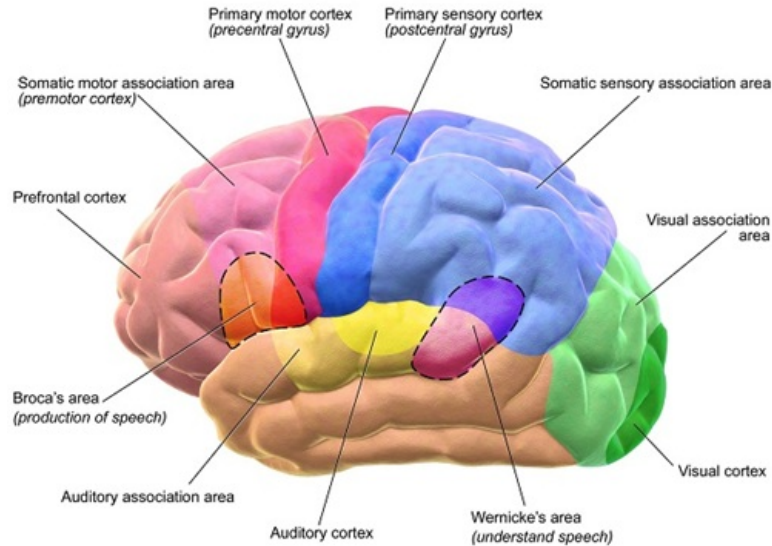


Figure 1.6: Functional areas of the cerebral cortex, [3]

### Brain stem and cerebellum

The brainstem and cerebellum are found in the posterior area of the skull (Figure 1.4). The brainstem is a small structure located in the hindbrain; it accounts for around 10% the total volume of the brain but contains about 50% of the total number of brain's neurons. It consists of the *mesencephalon*, the *pons* and the *medulla oblongata*; almost all cervical nerves originates from the brainstem. It plays a fundamental role in the regulation of sleep-wake rhythms and consciousness. The cerebellum is a bilateral symmetric structure; it is responsible of balance, motor coordination and motor control.

## 1.3 The regulation of motor control

As mentioned in section 1.1, paragraph *The spinal cord*, the cerebrum is contralaterally organized and one emispheres rules over the opposite side of the body. The correct execution of a volitional movement requires the integration of four factors (Figure 1.7):

- movement conception;
- realization of the motor program for the movement execution;

- movement execution involving the right muscles at the right time;
- constant feedback and presence of control mechanism.

Intention formulation and programming occur at the cortical level (*i.e.* along the cerebral cortex) and involves different areas: the supplementary motor area (SMA) in the frontal lobe, associative areas and the limbic system. The motor programming needs to be properly developed in order to guarantee an adequate muscular contraction; this happens in multiple functional areas of the cerebral cortex, such as the primary motor cortex (PMC), somatosensory areas, SMA, and pre-motor cortex – located in the frontal lobe, between the PMC and SMA. The program is then executed by the transmission of descendant signals to the right muscles; this happens through the activation of efferent neurons that innervate skeletal muscles: these neurons are called *motor neurons*. They are the only structures that control the contraction of skeletal muscles and are always excitatory. Two important descendant pathways that are involved in motor control are the *pyramidal* or *corticospinal tracts* and the *extrapyramidal tracts*.

### **Pyramidal tracts**

Pyramidal tracts, also said corticospinal tracts, are direct communication pathways between the PMC and spinal cord. The axons from which they originate are called upper motor neurons and the majority of these pathways cross over in the medulla oblongata (*cf.* section 1.1, *The spinal cord*). They are involved in the control of precise movements of the distal extremities of the superior limbs (forearm, hands and fingers).

### **Extrapyramidal tracts**

These pathways form indirect connections between the encephalon and spinal cord, *i.e.* neurons belonging to these tracts do not form synapses with motor neurons. These pathways influence the movements of the trunk, the neck and proximal segments of the limbs; in general, they are related to the coordination of large group of muscles, for example those involved in posture and balance control. The same holds for brain stem; in fact, it receives afferent signals – mostly deriving from sensory information – and adapts.

### **Basal ganglia and cerebellum**

After the motor cortex plans the movement and the signals are transmitted to the motor neurons, the cerebellum compares the real movement with the expected ones and, if discrepancies are met, it makes corrections in terms of force applied and direction. It is responsible for the maintenance of muscle tone during rest

and functions as *'living memory'*, storing information about previous movements so that they can be improved or perfected. In order to do so, the cerebellum receives continuous information from the motor cortex, sensory motor cortex, basal ganglia, brain stem and spinal cord and sends back information through the thalamus, so that the cerebral cortex can modify the afferent signals. Basal ganglia are a group of sub-cortical nuclei that perform a similar function: in fact, they provide feedback for the development of motor strategies and coordinated performance of motor tasks. They also play an important role in the execution of automatic motor tasks and in learning of repetitive motor tasks. By communicating with the cerebral cortex in the same way as the cerebellum, they allow to optimise volitional movements, inhibiting undesired acts.

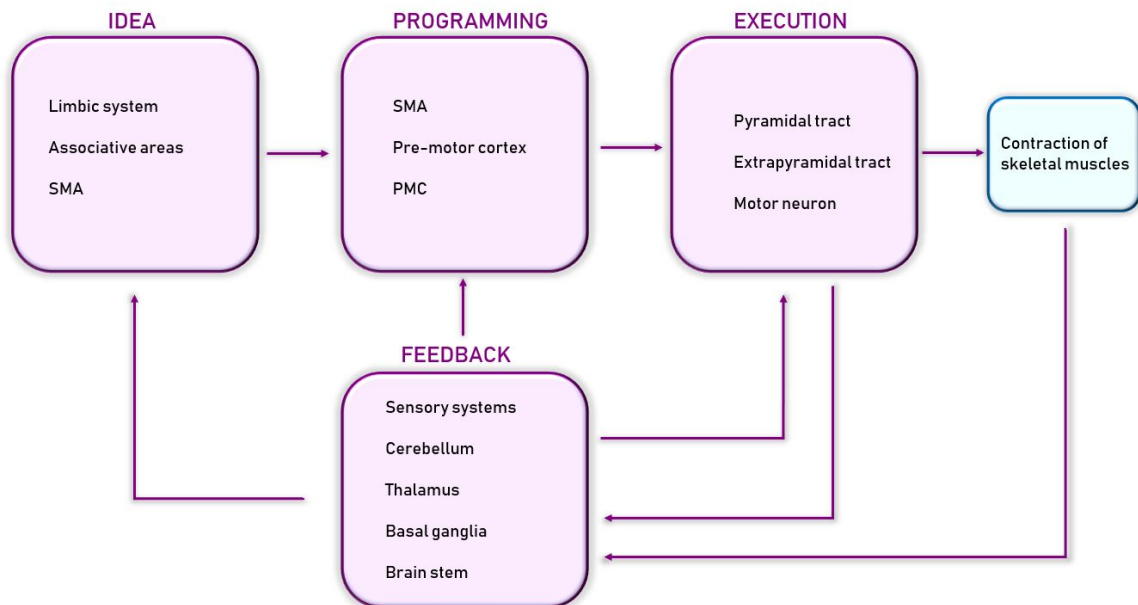


Figure 1.7: Processes that regulate the execution of voluntary movements. Volitional movements require the coordination of multiple nervous structures. The process begins with the movement conception (idea). Adapted from [43]

## Chapter 2

# Disorders of Consciousness

Disorders of consciousness are specific medical conditions that describe all the states in which the consciousness is inhibited. It consists of a wide spectrum of diseases that range from the *Locked-In Syndrome* (LIS) to the *Persistent Vegetative State* (PVS) or *chronic coma*. The term *consciousness* itself is not easy to be defined; in fact, it can be defined under different aspects, such as self-awareness, moral awareness and willingness to interact with the surrounding environment [46]. As Stuart Sutherland mentioned in the *Macmillan Dictionary of Psychology*, consciousness is defined as "*The having of perceptions, thoughts, and feelings; awareness Consciousness is a fascinating but elusive phenomenon: it is impossible to specify what it is, what it does, or why it has evolved*". Despite being a complex concept, it can be described by two main components:

- **Arousal**, associated with the regulation of consciousness, attention and alertness. In fact, the assessment of reflexes is an important factor to investigate the integrity of brain functions;
- **Awareness**, that is related to the functional integrity of the cerebral cortex and its subcortical connections.

Although recent biomedical techniques are applied in order to assess the extent of brain damage, consciousness cannot yet be measured quantitatively through the use of a machine; the Glasgow Coma Scale (GCS) is still largely employed: it is a neurological measurement scale that allows to assess the subject's level of consciousness. It consists of 6 different levels in which the visual, verbal and motor levels are evaluated. The lowest score is 1 (representing a patient in a vegetative state) and the highest 15 – representing a fully awake person.

## 2.1 Persistent Vegetative State

Persistent vegetative state is a disorder of consciousness that includes patients in a state of partial arousal that lied for at least 4 weeks in vegetative state; this syndrome can arise after traumatic brain injury (TBI) or non-traumatic events. The subjects suffering from PVS are typically unresponsive to the external environment, although at some levels of consciousness they may experience sleep-wake cycles or be in a state of permanent wakefulness. Furthermore, their eyes may be still or randomly moving and, under some circumstances, may track moving objects. The brainstem is usually intact, so this kind of patients can breathe autonomously and only needs life-sustaining equipment for feeding.

## 2.2 Minimally Conscious State

Minimally conscious state (MCS) differs from PVS in the fact that the subjects suffering from this condition have limited preservation of conscious self- and environmental awareness. Through the use of functional magnetic resonance imaging (fMRI) it was possible to demonstrate that MCS subjects show activation in auditory networks when hearing narratives of personal meaningful content, read by a familiar voice. Nevertheless, this kind of patients are not able to communicate properly.

## 2.3 Locked-in Syndrome

Locked-in syndrome is also known as *pseudocoma* and applies to the subjects that suffer from complete paralysis of voluntary skeletal muscles in the body, except for vertical eye movements – that are preserved. It is caused by damage occurring in specific portions of the brainstem, and the upper parts of the brain are intact. It is not uncommon that patients in the locked-in state are mistakenly diagnosed as persistent vegetative state (PVS) subjects, but they are in fact awake and aware of the surrounding environment but unable to communicate. Clinical varieties of the syndrome can be listed, such as *incomplete* LIS, that regards subjects that preserve some – even minimal – motor functions, and *transient* LIS, a condition that is likely to evolve towards partial or complete recovery. Nevertheless, one more clinical variety should be mentioned: the *total* LIS – or *completely* LIS (CLIS); in this case, where eye motor control is lost [46]. A similar condition can be found in anesthesia awareness, a medical complication that consists in a failure in the general anesthesia procedure, in which the subject wakes up during surgery and, though awake, is not able to communicate with the surrounding people.

# Chapter 3

## The EEG Signal

Electroencephalography is an electrophysiological technique used to monitor brain electrical activity. The first human EEG was recorded in 1924 by a German physiologist, Hans Berger; he carried on his predecessors' work and invented the electroencephalogram, the instrument with which the signal was recorded. The first observed signal was called *alpha wave* and was compared to an artificial 10 *Hz* trace to facilitate the analysis. From that moment on, several studies on brain activity have been conducted in medicine and psychology. The standard EEG method consists in a non-invasive approach; different electrodes are applied directly on the scalp and record over a period of time the spontaneous electrical activity arising from the brain. EEG is a technique that lacks in good spatial resolution but at the same time offers exceptional temporal resolution – around *ms* – and thus is largely used in diagnosis. In fact, it is employed to investigate epilepsy, sleep disorders, coma and brain death.

### 3.1 The International 10-20 System of Electrode Placement

The International 10-20 System of Electrode Placement is an internationally applied model that is used to correctly locate electrodes over the scalp during any EEG task. It was established in order to have standardized measurements and methods in the scientific community, and to guarantee reproducibility of clinical and research studies outcomes. The name 10-20 implies that the distance between adjacent scalp electrodes is, in terms of percentage, either 10 or 20 of a reference distance; the latter is measured as the total front-back or left-right semicircle perimeter.

One commonly used reference distance is measured from *nasion* to *inion*; the nasion is the depressed area below the forehead between the eyes, theinion is the occipital protuberance located in the lower area of the human skull. Each group of electrodes carries a label that indicates the area of the brain from which the biopotential is

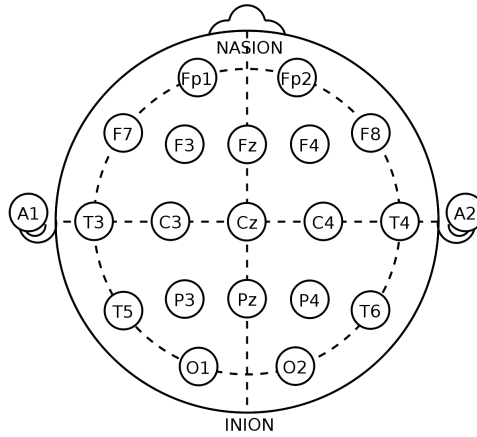


Figure 3.1: Electrode placement system according to the international standard

recorded, the principal are: FP (pre-frontal), F (frontal), T (temporal), C (central), P (parietal), O (occipital). Odd numbers refer to the left half of the skull and even numbers to the right half; Z-sites correspond to electrodes placed along the midline sagittal plane of the brain (Figure 3.1). Higher resolution systems as the one used in our research add accessory electrodes that fill the remaining areas according to the 10% division criterion. The Modified Combinatorial Nomenclature allows to label these intermediate recording sites: AF (between F and FP), FC (between F and C), FT (between F and T), CP (between C and P), TP (between T and P), PO (between P and O). It is important to notice that these new electrodes do not refer to an underlying area on the cerebral cortex, unlike the electrodes in IS 10-20 (Figure 3.2).

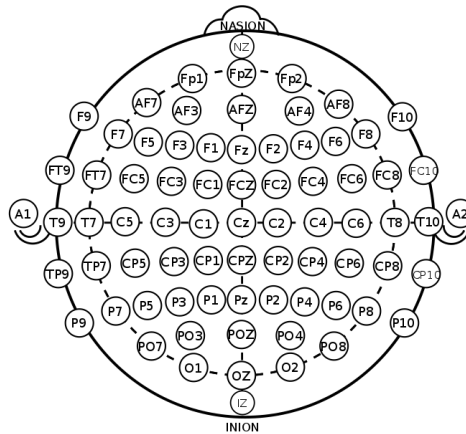


Figure 3.2: High-resolution electrode placement system according to the international standard

## 3.2 The EEG Rhythms

The brain electrical activity recorded during an EEG exam is very complex as it generates from different physiological areas simultaneously; for this reason, visual inspection sometimes may be hard. This is added to the fact that EEG signal amplitude of a healthy adult is around 10-100  $\mu V$ . Higher amplitudes – around  $mV$  – may be reached during subdural recordings, as happens in electrocorticography (ECoG), an invasive and not widespread technique. A commonly used approach is built on EEG frequency patterns, in fact brain electrical activity can be divided on specific frequency bands, (*cf.* table 3.1).

Biopotential	Frequency range
EEG signal	0.5 – 30 Hz
Auditory Evoked Potentials	100 – 3000 Hz
VEP	0.5 – 100 Hz
Event-related evoked potentials	0.1 – 30 Hz

Table 3.1: Different brain biopotentials and relative frequency bands, adapted from [11].

As regards physiopathological EEG signals, four main wave patterns can be distinguished [29]:

- Delta waves (**0.5 – 4 Hz**), are observed normally in infants and in deep-stage sleep in healthy adult subjects. It is a slow rhythm characterised by higher amplitudes. In non-healthy subjects delta waves may occur in case of subcortical or diffused lesions;
- Theta waves (**4 – 7 Hz**), are relatively slow waves normally observed in young children and represent drowsiness in healthy subjects. If present in awake adults they may be linked to subcortical focal lesions. Recent studies report increased theta activity in the frontal and prefrontal cortex is associated with deep meditation and tasks requiring attention and working memory [45];
- Alpha waves (**7 – 13 Hz**), the first waves to be ever recorded, they are predominant in the occipital regions of the brain. Their presence is related to relaxed or numb states and in early stages of sleep; alpha activity rapidly attenuates during attention-requiring tasks;
- Beta waves (**13 – 30 Hz**), are the dominant rhythm in healthy awake subjects. They are mostly observed in the frontal lobes of the brain and are associated with voluntary movements and motor control. They are significantly reduced in areas suffering from cortical damage.

Other two wave patterns need to be mentioned:

- Mu waves (**8 – 13 Hz**), partly overlapping with alpha waves, they can be mainly found in the frontal and prefrontal cortex. They reflect synchronous activity of motor neurons in resting states and are suppressed during voluntary tasks, suggesting neuron desynchronization during movement [35] [36] [34] [38];
- Gamma waves (**30 – 100 Hz**), are the fastest brainwaves. These wave pattern rests above the frequency of neuron firing and usually associated with anxiety states, stressful tasks or processing of information from different brain areas [21]

The main patterns are shown in fig.3.3.

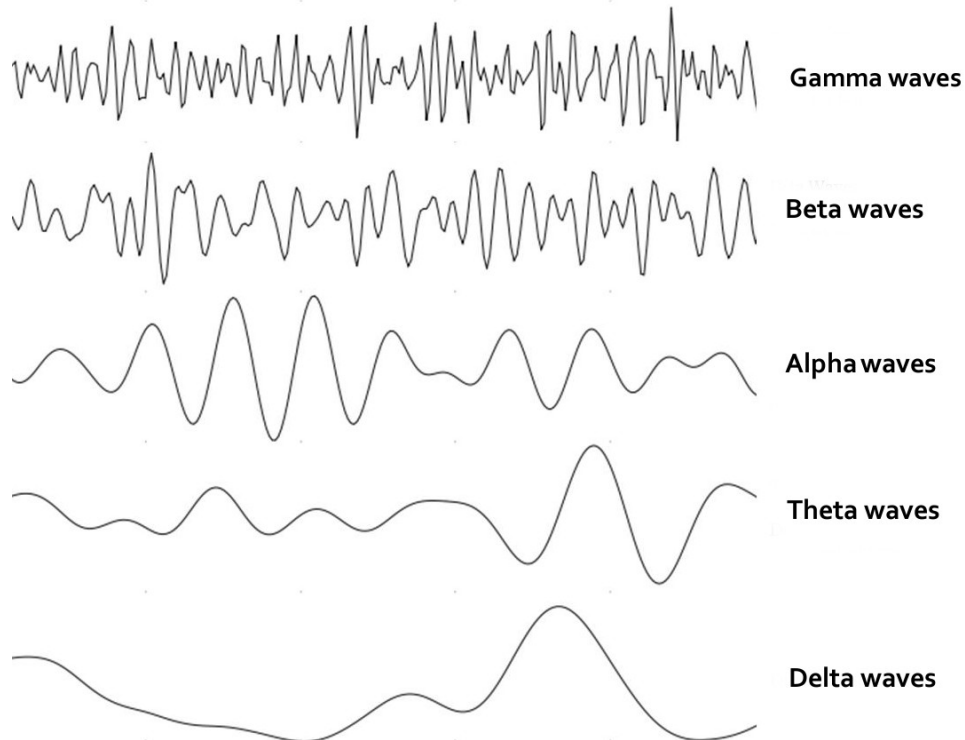


Figure 3.3: Principal brain wave patterns, ordered from highest to lowest frequency; adapted from [11].

### 3.3 EEG Artefacts

During any EEG recording, electrical signals of non-cerebral origin are also detected on the scalp. Given the low amplitude that characterizes the electroencephalographic biopotential, the so-called artefacts need to be rejected in order to proceed to a clear and precise data analysis. [30] Artefacts may be of biological and non-biological origin. [18] [19]

#### Eye blinking artefact

The bulbus oculi acts as an electrical dipole, where the cornea represents the positive pole – oriented anteriorly – and the retina the negative pole, oriented posteriorly. An alternate current is generated as the eyeball rotates around its axis, and it can be detected by nearby electrodes. As regards eye-blinking, the generated high-amplitude potential affects the EEG recording, especially in the FP area, causing symmetric downward deflections in the delta frequency range – with a power peak around 3  $Hz$ . The effect diminishes in more distant electrodes. [24]

#### EMG induced artefact

Electromyogram (EMG) activity from frontalis, temporalis, genioglossus and palatoglossus muscles is also recorded and affects EEG data. These artefacts are identified by means of duration, morphology and frequency components. In degenerative CNS disorders – such as Parkinson’s disease – EMG activity from tremor is found at frequencies overlapping the delta range.

#### ECG artefact and skin artefact

Electrocardiogram (ECG) artefact is quite common; nevertheless, this kind of artefact can be easily removed as it appears as regular periodic events and EEG recordings are not heavily affected by their occurrence. [16] [20] Skin artefact is due to the alteration of the physiological DC potential present between the stratum corneum and the stratum granulosum, due for example to skin tumefaction or sweating. It appears as slow-drifts and diminished signal amplitude.

#### Power-line artefact and electrode detachment

Both artefacts are non-biological and thus, not generated from the human body. Power-line artefact causes electrical interference at frequencies of 50 or 60  $Hz$ , depending on the local system. Sources of power-line noise may be cables and electronic devices working at low radio frequencies. Evidence suggests electrodes themselves may be sources of power-line artefact; anyway, they are responsible also for other types of abnormalities in EEG recordings, such as electrode pops or slow-drifts. The

former are short transients due to a sudden change in the electrode impedance; they are displayed as spikes. Slow-drifts, instead, originate from bad electrode impedance and may affect all channels involved in the recording if the difect comes from the reference electrode.

#### **EEG artefact removal: an approach**

Recent studies report Indipendent Component Analysis (ICA) as an effective method for artefact rejection, this may lead to two different approaches. The first relies on the elimination of the entire trial, carried out by visual inspection or threshold-based methods. A more automatic approach splits the trial into components, and aims at isolating the artefact in order to reject it. The method proved to be effective in ECG and eye-blinking artefacts removal [10]. ICA may be also used to reject EMG artifacts and electrode pops, though the former can also be corrected in some particular situations by implementing a proper low-pass filter. [30]

# Chapter 4

## Event Related Potentials

As described in the previous chapter, the EEG was invented and used, to this day, in order to record the electrical activity arising from the brain; thus, it proved itself to be an excellent tool for monitoring and diagnosis. Alongside conventional EEG recording, where brain activity is observed under normal or pathological circumstances (such as epilepsy seizures) over a period of time, it is possible and much used in contemporary clinical studies to use certain activation procedures. These consist in eye closure, visual or acoustic stimuli, meditation and other mental tasks; they are useful to let emerge specific EEG activities that could not be seen otherwise: they are called event-related potentials (ERP).

### 4.1 Introduction

Event-related potentials are very small voltages generated in brain structures in response to specific events or stimuli (*Blackwood and Muir, 1990*). They are changes in physiological EEG activity that occur time-locked to sensory, motor or cognitive events and provide a non-invasive approach in clinical and research neuropsychophysiological studies. In fact, ERPs are widely used in neuroscience and cognitive science. Just like conventional EEG traces, ERPs are characterised by low spatial resolution and high temporal resolution; they are described in terms of amplitude and latency, that is the time at which the amplitude reaches 50% of peak amplitude. Classic ERP waveforms consist of a sequence of positive and negative deflections which can be sorted into different components.

### 4.2 Components

Conventionally ERPs are divided in two main categories, which represent the early and the late parts of wave; the former are called *exogenous* (or sensory), since they depend only on the physical factors of the stimulus, the latter are said *endogenous*

(or cognitive) since their occurrence depends on the level of consciousness of the subject and they are related to cerebral processing. [44] Apart from these two main classes, there are different kinds of ERPs, to which the scientific community usually refers to by means of acronyms: for example, the letter (P or N) represents the polarity, the number represents the latency characterizing the potential, expressed in *ms*. (Fig. 4.1) The main waveforms employed in clinical studies are P50, P300, CNV and MRCP; the last one will be of great interest in this research work and thus described in detail in a dedicated subsection.

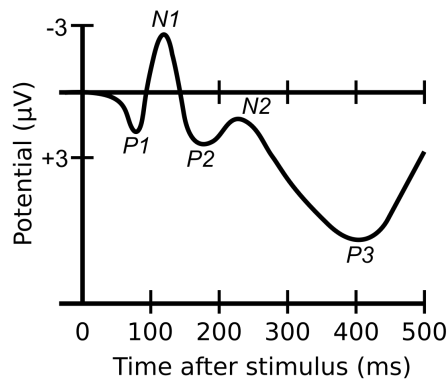


Figure 4.1: Example of event-related potentials, with different positive and negative components, [48].

### 4.2.1 P50

P50 is a positive deflection occurring about between 45 and 75 *ms* after the stimulus (usually auditory). The amplitude can be measured as the difference between the potentials peak and the preceding negative deflection (*Clementz et al, 1997*), in absolute terms. It is examined in order to describe the neural processes by which the brain filters redundant information, grouped in the term *sensory gating*. This kind of potential is elicited, for example, during the paired-click paradigm: the subject is presented with one auditory click, followed by another one at a maximum distance of 500 *ms*. The cognitive response to the second stimulus is normally reduced, resulting in a P50 suppression, because the signal is perceived as redundant. This test fails in subjects suffering with schizophrenia, ADHD or ASD.

### 4.2.2 P300

P300 - also found as P3, fig. 4.1 - is a positive ERP component and is also the one most research work is dedicated to. It is considered to be a cognitive potential, since it depends on the subjects reaction to the stimulus provided and is found mostly in the parietal lobe. It was first discovered by Sutton et al. and the latency is around

250-400 *ms* – in healthy subjects of age 20 to 70; it is related to processes involved in the stimulus evaluation and thus is believed to be an attention-dependent cognitive component in wakefulness. It can be found through the *oddball paradigm*, that consists in providing the subject with a series of stimuli, where one of them occurs only occasionally – the oddball. The subject is requested to identify the target stimuli by responding only to the infrequent ones. The amplitude of P3 depends on the subjects attention (high levels originate higher amplitudes) and the latency reflects the speed of stimulus classification: the shorter the latency, the higher the mental performance. [44]

### 4.2.3 Contingent Negative Variation

Contingent negative variation, known as CNV, was discovered around the same time as P300. It consists of two components: the early component indicates the arousal process while the late component is an indicator of the attention used during the experimental task. The elicitation process is based on the Standard Reaction Time paradigm (SRT), in which the subjects are requested to respond – physically or mentally – to a certain number of external stimuli; the cues may be random or presented with a certain predictability. It was observed that the CNV is actually elicited after about 30 trials of paired stimuli; the peak occurs at about 250-450 *ms* and has a maximum amplitude of 20  $\mu V$ . The peak rises slowly when the subject seems to have assimilated the task, while it rises abruptly in those situations where the subject has no expectation. In fact, in recent studies CNV has been associated with expectancy; Walter et al. have noticed that the electrical response is attenuated when a single cue is repeated, meaning that the subject is less responsive as the order becomes a habit. In this perspective, it was also demonstrated that the potential is attention-dependent, since the amplitude rises again if the experimental protocol is changed during the trial without the subject knowing.

## 4.3 Movement Related Cortical Potentials

Among negative event-related potentials we also find movement related cortical potentials: they are time-locked to a specific event, that is the onset of a voluntary movement [39]. These potentials occur in a time interval that may be prior or subsequent to the actual performing of the movement. The first successful report of brain electrical activity before voluntary movement was recorded in 1964 [26]; other studies tried to identify this kind of potential before but proved unsuccessful and managed to pinpoint only post-movement activity – probably due to low SNR [8]. In order to make the activity emerge, Kornhuber and Deecke recorded simultaneously EEG and EMG while the subjects were repeatedly making voluntary movements at self-paced velocity. The EEG data was averaged off-line, taking into account as

epochs the samples preceding the EMG onset. This allowed to identify the two main components of the MRCP: the Bereitschaftspotential (BP), to which one can refer to as Readiness Potential (RP), and the Reafferent Potential. Two more components need to be mentioned – and are found just before the movement onset: pre-motion positivity (PMP) and motor potential (MP) [15]. The physiological significance of MRCP and its components is still going under research. The readiness potential is the main matter of attention in this study and is described in detail in the following chapter.

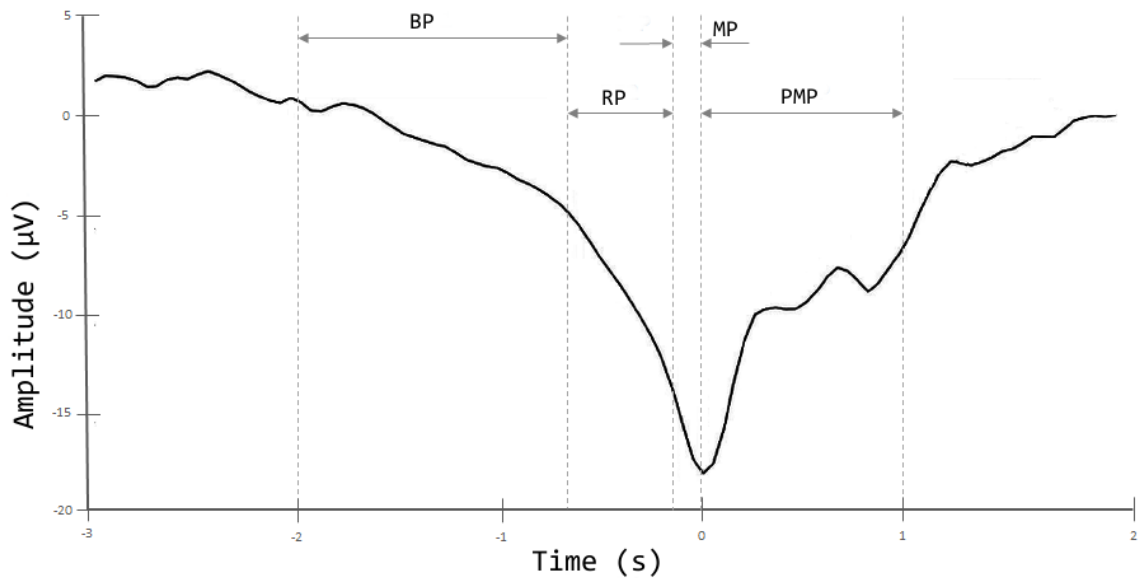


Figure 4.2: Movement related cortical potential and its components: readiness potential (BP), reafferent potential (RP), motor potential (MP) and pre-motion positivity (PMP). Adapted from [47].

# Chapter 5

## Bereitschaftspotential

As previously introduced (see chapter 4.3), the Bereitschafts potential – from the German ”*willingness, readiness*” – is a gradual decline on EEG averaged data, that occurs at most 2 s before any volitional movement. It is a very small potential: the maximum amplitude is set around 20  $\mu V$  but it is usually found at values of 5 or 10  $\mu V$ ; it is found largest in the centro-parietal area but is well distributed all over the scalp, regardless the site of movement. It is demonstrated that in experimental settings in which the subject acts at a self-pace rate of 5 s or longer, the BP starts earlier compared to those tasks in which the subject performs the action following an external cue – this is due to the fact that in the first case the subject has more time to prepare for the movement. As mentioned before, the identification of BP is difficult most of the time, both because of the very small amplitude (around 100 times smaller than the alpha-pattern amplitude) and because the EEG signal is highly affected by noise, making it difficult to have a good SNR.

### 5.1 Components

The readiness potential can be analysed in terms of two separate components: *early BP*, beginning about 2 s before EMG onset in the supplementary motor area (SMA, cf. section 1.2), and *late BP*, occurring in the primary motor cortex and premotor cortex (cf. section 1.2) about 400 ms before movement onset (Figure 5.1). While the early component is fundamentally a slow segment, the gradient increases abruptly in the late component: due to this fact, it is also called *Negative Slope* (NS<sup>+</sup>). Since its occurrence may vary due to different factors (subject, attention, task, ...), it is more easily found by comparing the gradient of the analysed segment than by setting a starting time (e.g. 500 ms before EMG onset). The late BP is maximal on the contralateral central area for hand movements and at the central sulcus for foot movements. Initially, the early component was thought to represent the preparation for the movement and the late BP was thought to represent the actual site where

the movement is generated; however, the early BP may also be considered to be site-specific, at least as far as the SMA is concerned. Moreover, the late component, when unilateral hand movement is performed, features asymmetric distribution. This has brought up studies about the *lateralized readiness potential* (LRP), that is obtained by subtracting from C3 potential the potential at C4, for both left- and right-hand movement. It is better obtained in choice reaction time task than in self-paced motor tasks.

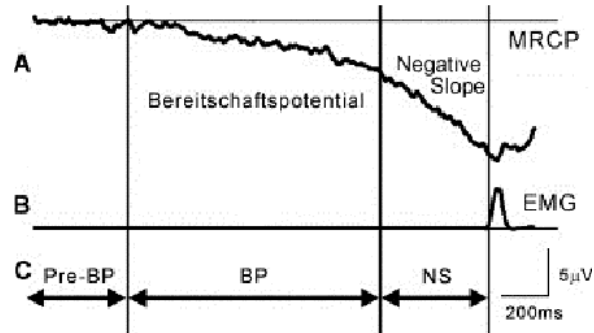


Figure 5.1: Bereitschaftspotential (or readiness potential) and its fundamentals: early component (BP), late component (NS'). The EMG onset is also shown as well as the pre-readiness potential (Pre-BP). [12]

## 5.2 Influencing factors

As mentioned in the introduction section of this chapter, the time occurrence of the readiness potential recorded in a self-paced condition may vary; the same holds for the amplitude. These two parameters are largely influenced by different factors, among which:

- level of intention;
- preparatory state;
- movement selection (free or fixed);
- learning and skill acquisition;
- velocity of repetition;
- precision of movement;
- perceived effort;

- force exerted;
- pathological lesions of different brain structures.

It is important to notice that so far the studies about MRCPs revolved around simple motor tasks such as foot or wrist extension, fist clenching or elbow movements, finger extension (as in the case of this report); all these tasks are precise and very different than those performed under natural conditions and thus must be treated differently. The influencing factors and their effects are summarized in table 5.1. Starting by analysing the case of the force exerted, larger amplitude is found in the last 100 *ms* segment of BP, with greater perceived effort than the force itself. During different tasks comparison it was also demonstrated that movements requiring precision in terms of force applied resulted in higher amplitude BP than simple tasks [41] [28]. The movement velocity also affects the starting time and amplitude of BP; in fact, as said before, the faster the movement, the later the BP occurs – that is, the closer to the EMG onset. Two other noteworthy factors are complexity of the movement and discreteness. As regards complexity, it was demonstrated that the amplitude of the BP increases when two tasks are paired, compared to the magnitude found in the single tasks respectively [9]. In support of this study, two tasks were compared: the first involved the simultaneous extension of the middle and index finger, the second task consisted in the sequential movement of the two mentioned fingers, so that the muscles involved in the two tasks were the same. As a result, a larger amplitude of late BP was found in the sequential task, and it was observed in the SMA as well as the sensorimotor cortices, suggesting that also the latter play an important role in the preparation of complex movement. This activation pattern was also confirmed by a CBF activation study with positron emission tomography (PET) [23] [40]. As for discreteness, Kitamura et al. [22] compared a simultaneous finger movement task to an isolated finger movement. Larger magnitude of the late BP was found in the latter, even though the number of muscles involved was significantly lower. The fact that in discrete and complex tasks the late component of the readiness potential meets an important increase may suggest the fact that, when performing studies on motor control or on its abnormalities in pathological conditions, the task complexity or subjective difficulty needs to be taken into account as important influencing factor.

### 5.3 Generator sources

Different techniques have been applied in order to localize the dipole source of MRCPs. As regards hand movement, the main generator sources are thought to be SMA and lateral precentral gyrus – both bilaterally. Furthermore, in [37] it is demonstrated that only the current source identified in SMA is affected by how the movement is selected. The readiness potential actually occurs earlier in the medial

<b>Factor</b>	<b>Early BP</b>	<b>Late BP</b>
Intention	Larger*	
Preparation	Earlier onset*	
Movement selection	Larger	No effect
Learning	Larger during learning	No effect
Force exerted	Larger*	
Speed	Later onset*	
Precision	No effect	Larger
Discreteness	No effect	Larger
Complexity	No effect	Larger
Cerebellar lesion	Small	Small

Table 5.1: Influencing factors in readiness potential early component (early BP) and late component (late BP), adapted from [39]. \* means that there are no clearly established effects on the late BP.

SMA, then in the contralateral primary motor cortex (PMC) and finally in the ipsilateral PMC, as shown in figure 5.2. However, because of the anatomical variability of the SMA in different subjects (in some cases it can reach the crown of the superior frontal gyrus), the scalp recording of the actual electrical brain activity may not be certain. In order to have a more precise location for activation patterns, some studies implemented magnetoencephalography (MEG), a functional neuroimaging technique used for mapping brain activity that records magnetic fields that occur naturally in the brain [49]. It is important to notice that MEG only records the components that are tangentially-oriented to the head surface, whereas EEG records both tangentially- and radially-oriented components. The negative potential in MEG begins later than that of EEG and is located mostly over the contralateral central region; the explanation to this is found in the fact that early BP starts bilaterally but is recorded only by EEG because it is radially-oriented, whereas late BP is recorded both by MEG and EEG due to its tangential orientation and occurs contralaterally in the PMC. This suggests the fact that also SMA contributes to the preparation of volitional movements; in particular, SMA activity proved to be contralaterally predominant.

## 5.4 Free will and Libet's experiment

Kornhuber and Deecke [26] studies paved the way for studies concerning neuroscience of free will. Though up to now this research field remains controversial, several experiments have been made, studying the brain and its decision-making processes, moral responsibility and consciousness. The pioneer of human consciousness studies

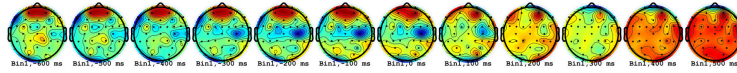


Figure 5.2: Generation of volitional movement in the supplementary motor area and primary motor cortex; the late BP is contralaterally generated around 300 ms prior to movement.

was Benjamin Libet, a researcher in the physiology department of UCSF. In 2003, he was the first to ever win the *Virtual Nobel Prize in Psychology*, for his '*pioneering achievements in the experimental investigation of consciousness, initiation of action, and free will*'. In 1983 Libet, alongside with his research fellows, carried out a series of experiments aiming at identifying the exact moment in which the subjects became aware of their decision making. Libet's experiments required the subject to be sitting at a desk, in front of an oscilloscope timer (*Libet's clock*); this special clock was designed using a cathode ray oscilloscope and had a single light dot revolving in circular motion, mimicking the movement of the second hand of an actual clock (Figure, 5.3). The subjects were required to randomly flick their wrist while their electrical brain activity was recorded; in addition, Libet and his research group asked the subjects to look at the light dot and report the exact position when they had felt the will to move the wrist. Libet found that, although the consciousness of the

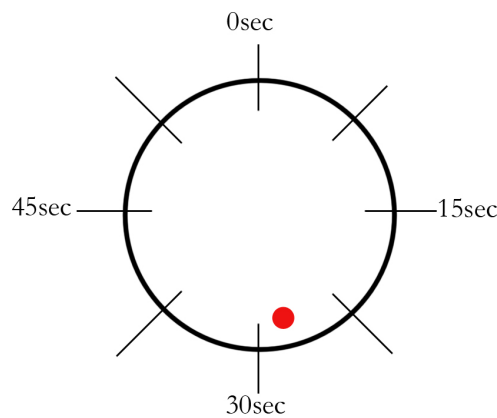


Figure 5.3: Libet's oscilloscope timer, [4]

decision came only 200 ms before movement onset, the early BP component came about 1.5 s before action and the late readiness potential component occurred around 550 ms before the motion started (Figure 5.4). Moreover, *unconscious* activity to flex the wrist occurred about 300 ms before reporting *conscious* awareness of decision making (Figure 5.4). As a result, Libet found that conscious decisions are

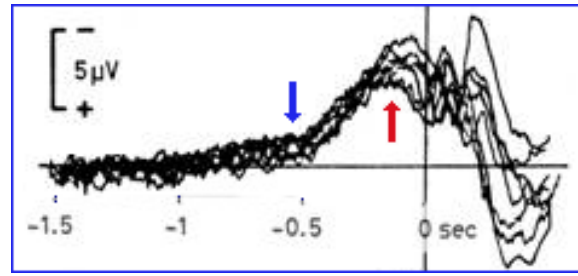


Figure 5.4: Bereitschaftspotential recorded during Libet's experiment; the blue arrow represents the rise of BP and the red arrow represents conscious awareness of decision making, [4]

preceded by unconscious brain activity – about 500 *ms* before. This suggests that any voluntary decision made by a subject derives from a subconscious level and is later translated into conscious will.

## 5.5 Outcomes

Volition has traditionally always been associated with human freedom. As introduced in section 5.4, the field of Neuroscience is trying to determine how voluntary actions originate and the role of consciousness in their production. Although Libet's experiments were both applauded and criticised, it is very unlikely that a single study is able to disprove historical belief of free will. In fact, up to now definitions of consciousness still vary and each one must be taken into account singularly and examined depending on the experimental and empirical background. What is true, though, is that several physical and electrical factors are involved in human decision making; our intent is to explore the field of movement related cortical potentials – especially the readiness potential – in order to find evidence of consciousness in voluntary and semi-voluntary movements.

# Chapter 6

## Materials

In the following sections are illustrated all the materials employed in the clinical study – including data recording instrumentation and the acquisition software – and the experimental protocol that was applied.

### 6.1 Experimental Protocol

The experimental analysis was carried out in Turin, at *Centro Puzzle*, a rehabilitation daytime centre for people suffering from traumatic brain injury (TBI) and acquired brain injury (ABI); our research team included biomedical and electronic engineers, medical doctors and neuropsychologists. The clinic provided the team with proper instrumentation for EEG recording in a dedicated space; the clinical study involved both healthy and injured subjects and data was collected in three different stages.

#### 6.1.1 Stage one

The first acquisition involved 27 healthy subjects, of age 20 to 26; 13 performed the acquisition blindfolded, so as to reduce noise coming from the occipital region of the brain (*cf.* section 1.2, *Cerebral cortex and functional areas*). The experimental protocol consisted of two specific tasks, voluntary and involuntary respectively, that were carried out by the subject sitting on a chair, in front of a computer monitor:

1. **First task, voluntary:** the subjects were asked to keep their right hand palm-up, placed on their right leg. By looking at a watch on screen <sup>1</sup>, they had to quickly bend their right index finger every 10 s.

---

<sup>1</sup>The blindfolded subjects responded to an acoustic signal that occurred every 10 s.

2. **Second task, involuntary:** the subjects were asked to look away from the computer monitor; during the recording time a trained experimenter evoked the *patellar tendon reflex*.

EEG and EMG (from the hand and the leg) were recorded during the acquisition at a sampling frequency of 512 *Hz* and each task consisted in 40 trials. For the EEG acquisition only 7 scalp electrodes were used, positioned according to the IS 10-20 (*cf.* section 3.1) over the pre-frontal, frontal, parietal and occipital cortex. The electrodes were Cz, C3, C4 for the central lobe, FCz, FC3, FC4 on the frontal lobe, Pz on the parietal lobe and Oz on the occipital lobe, used also as reference electrode. As regards hand-EMG, one electrode was positioned on the metacarpal portion of the index finger (above and below the *flexor carpi radialis muscle*) and another one placed on the wrist functioned as reference electrode; the EMG response to patellar tendon reflex was recorded using one electrode on the medial portion of the *rectus femoris*, while the reference electrode was placed on the ankle.

### 6.1.2 Stage two

The second dataset acquisition involved 18 healthy subjects (9 females, 9 males) of age 22 to 60. The subjects were sitting on a chair, facing a blank wall and all blindfolded with a soft eye sleeping mask. They had to perform 40 trials of three different tasks: completely voluntary, semi-voluntary and involuntary, respectively.

1. **First task, completely voluntary:** the subjects were asked to keep their left hand, palm-up, placed on their left thigh. After hearing an acoustic signal, they had to decide the moment in which they would move their left index finger and move it;
2. **Second task, semivoluntary:** keeping the same posture and position, the subjects were asked to bend the index finger as soon as they had heard the acoustic signal;
3. **Third task, involuntary:** while the subjects sat still, their legs dangling from the chair, a trained experimenter evoked the patellar tendon reflex.

During the acquisition scalp EEG and EMG were recorded, at sampling frequency of 512 *Hz*. As regards EEG data, the employed channels were now 34, positioned according to high-resolution IS 10-20 (Figure 3.2), with ear-lobes used as reference. Electrical activity from the eyes was also recorded, in order to easily remove eye-blinking artefacts (*cf.* section 3.3); the electrodes were applied above the eyebrow and on the external side of the orbit, in order to record activity from *levator palpebrae superioris* and *lateral rectus* muscles. This time, EMG was recorded only in task 1 and 2, in order to establish movement onset and determine when the readiness

potential occurred (*cf.* section 5). The completely involuntary task was performed in order to find the differences in voluntary and involuntary movements generation, with a view to a subsequent implementation in injured subjects.

### 6.1.3 Stage three

The third dataset acquisition was performed in order to perfect data cleaning and pave the way for the aim of this research work, *i.e.* looking for a correspondence between habit and BP's amplitude abatement and late occurrence. In this stage, 6 subjects were involved, 4 females and 2 males; the tasks were only two and corresponded to the completely voluntary and semivoluntary tasks of stage 2 (*cf.* section 6.1.2), and consisted in 40 trials each. The EEG and hand-EMG montages were the same as the previous acquisition; the only exception was made for EOG recording, that was performed with 7 electrodes: two above the eyebrows, two on the external side of the orbit and one taken as reference for both eyes placed on the *nasion*. In this last acquisition also an injured subject was involved; he was a 40 y.o. male suffering from TBI, in minimally consciousness state (MCS). The experimental protocol adopted in this case is different and described in the following section.

### 6.1.4 Experimental protocol in injured subjects

This experimental work led also to the creation of a new protocol, dedicated only to injured subjects. The document is strictly confidential and contains all information regarding the people in charge, the involved institutions and personnel, patient enrolment, medical equipment, motivations of the study, experimental protocol, objectives and expected results. Once the document is complete in all its parts, it will be submitted to the ethical committees of Local Health Corporations. The following sections report some of the parts, as an example.

#### Patient enrolment

The clinical study is reserved for subjects suffering from disorders of consciousness, such as MCS and LIS. They shall be enrolled from medical facilities participating in the project and be authorized by their legal representative. The sample should be made at least of 20 subjects, of age 20 to 50. Exclusion criteria are:

- Pacemakers, DBS, cochlear implants;
- Scalp dermatitis or large scalp scars;
- Allergies to alcohol-based products or abrasive gels;
- Presence of cranial ferromagnetic prosthetic elements;

- Inconvenient neurological conditions (EEG signal alterations, epilepsy, ...).

### Experimental procedure

The subjects will be laying down on a medical stretcher and always accompanied by a caregiver and a nurse (or instructed healthcare operator). A trained experimenter will place on their head a fabric EEG headcap, available in different sizes, and perform skin and electrode preparation. The electrode placed on the occipital area of the brain will be disregarded for two reasons: most of the subjects keep their eyes constantly open and visual noise would saturate the other interesting channels; the subjects position makes it difficult for the operator to perform accurate skin preparation on the posterior portion of the head. EMG signals from the hand and leg are recorded too. The task is carried out as follows:

- **First trial:** the caregiver<sup>2</sup> will ask the subject to *move* a specific limb at a specific time, by using different verbal stimuli (such as "*If you can hear me, please raise your hand*", ...);
- **Second trial:** the caregiver will ask the subject to just *imagine* to move a specific limb, following the same verbal instructions as before.

Invalid trials – such as, the subject during the recording is moved accidentally by the people who surround him – are marked by the experimenter with an apposite device (*cf.* section 6.3.4) and discarded. The trial can be put to an end any moment according to the caregiver or medical staff.

### Medical data regulations and documents

All data coming from the trials has to be anonymized in order to protect the subjects' personal and confidential details and to allow the distribution of data for scientific and clinical reports – under permission of the Clinical Study Supervisor. The subjects' caregivers will be provided with an *informed consent* that guarantees the correct use of the collected data. Furthermore, the document describes the aim of the clinical study, the potential medical risk (in our case, minimal) and the subjects and caregivers' legal rights. The last document that is attached to the experimental protocol is the Declaration of Helsinki, that is considered the cornerstone document on human research ethics. By agreeing on this declaration, the experimenter commits to respecting the subject as an individual from the beginning to the end of the study and commits to put the subject's welfare over the interests of science and society. Ethical considerations must always come before laws or other regulations.

---

<sup>2</sup>Or the nurse, in case the caregiver is not present.

## 6.2 Data anonymization

A very important process at the end of experimental acquisition work was data anonymization, that consisted in removing all personal and identifiable information from our three data sets, according to European Union’s new general data protection regulation (GDPR), that affects also medical data. The anonymization protocol was developed together with the Centre for Neuroscience & Cognitive Systems at Italian Institute of Technology (Rovereto, Italy) and consisted in associating each subject with an 8-characters label, in which name, surname, acquisition date, year of birth and sex are encrypted. In addition, other two labels were added, representing stages one and two of the dataset acquisitions.

The data were codified as follows (Figure 6.1):

- **Name and surname:** the first two characters in the label represent the first letter of the name and the first letter of the surname (in order);
- **Acquisition date:** the third character in the label is a number and represents the last digit of the year of acquisition. The month of acquisition is registered in the sixth and seventh characters. Months are represented by two digits in temporal and cardinal order (01 → January, . . . , 12 → December);
- **Year of birth:** the fourth and fifth characters in the label are numbers and represent the last two digits of the subject’s year of birth;
- **Sex:** the subject’s sex is registered in the eighth character; 0 is associated with males and 1 with females.

In addition, as mentioned before, it is possible to specify whether the collected data belongs to the first acquisition (indicated as **VM**) or to the second acquisition (indicated as **VP**). As an example, the fictitious character Jane Doe, born on December 31<sup>st</sup>, 1999 and undergoing the tasks on January 1<sup>st</sup>, 2020 will be represented as JD099011. If she had participated in the first dataset acquisition, the label would have been JD09901\_VM, whereas if she had took part in the second dataset acquisition it would have been JD099011\_VP.



AA12345X

Figure 6.1: Example of the label created for data anonymization. In order: subject’s initials (red), year of acquisition (blue), year of birth (green), month of acquisition (pink), sex (orange).

## 6.3 Hardware

All biomedical instrumentation and equipment were supplied by Centro Puzzle; the employed materials include skin preparatory materials and electronic data acquisition equipment.

### 6.3.1 EEG caps and skin preparation

Two different EEG caps were used during trials; in the first dataset acquisition (*cf.* section 6.1.1) it was employed a standard silicone EEG cap, resizable, that could be used with bridge electrodes (Figure 6.2). This cap ensured strong electrode adherence – resulting in good quality signals – but it was impossible to implement a high-resolution system. From the second acquisition, data were collected with a pre-wired fabric headcap (Figure 6.3), produced by EBNeuro, which allowed high-resolution recording, with 34 scalp electrodes and the possibility to record also ECG data for further data cleaning (*cf.* section 3.3). The scalp, under normal conditions, is characterised by an impedance (for  $cm^2$ ) of about  $10\text{ k}\Omega$ , thus, in order to have a clean trial the skin needs preparation. Different procedures were followed during the acquisitions. Only in the first stage of data collection, when the silicone headcap was used, TEN20 conductive paste was employed to keep the bridge electrodes in place and guarantee clear recording. From the second dataset acquisition on, the scalp was first gently rubbed with NuPrep, a skin preparator gel that contains mildly abrasive factors that help removing the outermost layer of the skin, thus lowering impedance and enhancing recording performance. Secondly, each electrode site was filled with a conductive electroencephalography gel. The best effect was obtained in the injured subject: all electrodes resulted in having very low impedance. This is also due to the fact that humid and perspiring skin has lower impedance (*cf.* table 6.1). No skin preparation was made for EMG electrodes, since they were placed in all three acquisition using TEN20 conductive paste.



Figure 6.2: Standard EEG silicone cap used in the first dataset acquisition, [2]



Figure 6.3: EBNeuro’s pre-wired headcap employed in the second dataset acquisition.

Skin condition	Impedance for $cm^2$
Wet, perspiring	1 $k\Omega$
Dry	10 $k\Omega$
Dry and callous	100 $k\Omega$

Table 6.1: Approximate values of contact impedance between the skin and a metallic electrode under three different conditions. Adapted from [25]

### 6.3.2 Electrodes

As previously introduced, the employed scalp electrodes were of two types: bridge electrodes and cylinder-shaped electrodes – covered in polymeric material. However, both types consist in Ag/AgCl electrodes, highly recommended for this kind of application, due to their low half-cell potential (about 200  $mV$ ) at room temperature that guarantees low impedance. The electrodes used for EMG and EOG recording were self-adhering electrodes and cup-electrodes, the latter were positioned using TEN20 conductive paste.

### 6.3.3 Amplifier

The amplifier used for the recording is included in Mizar Sirius System and is part of EBNeuro’s Galileo Patient Management System (Figure 6.4). The amplifier, called *Brain Explorer*, provides a high number of channels (AC/DC) and supports sampling frequencies up until 32  $kHz$ . It features high sensitivity also for large dynamics and high CMRR. The parameters set for the acquisition are listed in the following sections.



Figure 6.4: Galileo NT workstation, part of EBNeuro. It includes a digital amplifier and a signal-processing software. [6]

### EEG recording

The parameters were chosen according to EEG frequency bands and its expected amplitude; the amplifier allowed to set early stage filters in order to facilitate further data cleaning.

- **Sampling frequency:** 512  $Hz$ ;
- **Notch filter:** 50  $Hz$ ;
- **LPF cut-off frequency:** 45  $Hz$ ;
- **HPF cut-off frequency:** 0.015  $Hz$ ;
- **Amplitude range:**  $\pm 10$   $mV$ .

### EMG recording

The parameters set for EMG recording are the following:

- **Sampling frequency:** 512  $Hz$ ;
- **Notch filter:** 50  $Hz$ ;
- **LPF cut-off frequency:** 400  $Hz$ ;
- **HPF cut-off frequency:** 5  $Hz$ ;
- **Amplitude range:**  $\pm 70$   $mV$ .

### 6.3.4 Acoustic signal generator and Pushbutton Pad

The acoustic signal generator consists in a software created with **Opensesame** using high-level programming language Python, in which the experimenter chooses the type of the trial from a simple and user-friendly GUI (Figure 6.5). Depending on the trial selected, the software generates a series of audio cues that are heard from the subjects and are later converted into voltage signals through the DAQ *LabJack U3-LV*, in order to synchronise them with the electroencephalographic traces.



Figure 6.5: Opensesame GUI used by the experimenter.

The pushbutton pad is an electronic device based on a textitvoltage divider circuit that works as a voltage impulse generator. Every button corresponds to a different voltage level (Figure 6.6). The equipment sends to the amplifier voltage impulses value in order to mark the trials as *good* or *not valid*. For example, if healthy subjects talk or move their head during the acquisition, the trial is considered not valid; as for injured subjects, the trial is invalid when they are moved by the caregiver or the healthcare professional in charge.



Figure 6.6: Pushbutton pad; each button corresponds to a different voltage value.

## 6.4 Software

The software used in data acquisition and data processing were, respectively, the embedded software provided by the GalileoNT workstation and EEGLAB, a plugin implemented in MATLAB®. The latter is developed by MathWorks and is the chosen environment in which further data analysis was carried on during this research work.

### 6.4.1 Galileo Suite

*Galileo Suite*, provided by EBNeuro, is the software dedicated to the acquisition and exportation of EEG trial data. When launched, the wizard interface asks the user to insert personal data of the subject (name, surname, DOB, anamnesis) and then proceeds to the recording environment. At this moment, it is possible to check the scalp impedances (Figure 6.7); it is recommended to perform this check while preparing the skin (*cf.* section 6.3.1), so that adjustments can still be made. Right before the start of the trial it is possible to make some visual improvements, like: implementing better highpass or lowpass filtering, changing the dynamics so that the signal looks better on screen, hide channels that are not of interest. All this adjustments are canceled once the trial is exported to a raw file, and only the initial parameter settings are kept (*cf.* section 6.3.3).

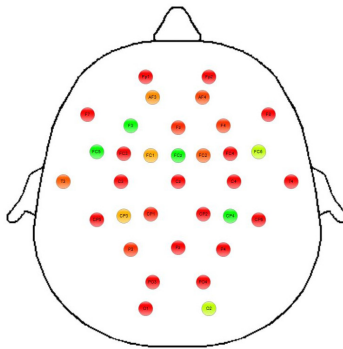


Figure 6.7: Scalp electrodes during calibration. The threshold was set at  $1\text{ k}\Omega$ ; red, orange and yellow dots are above that threshold and green dots are below – meaning the impedance is good.

At the end of the acquisition, the experimenter is able to export files to different formats, including `.edf`, `.set` and `.asc` (the preferable choice); at that moment one must choose the sampling frequency of the collected data and which channels are to keep.

## 6.4.2 EEGLAB

*EEGLAB* is an interactive MATLAB® toolbox, developed by the Swartz Center for Computational Neuroscience (UC, San Diego). This tool is characterised by an interactive GUI that allows the user to process high-density EEG data (Figure 6.8); it offers ICA algorithms, as well as time-frequency analysis and standard averaging methods. To the purpose of this research, *EEGLAB* was used to perform initial

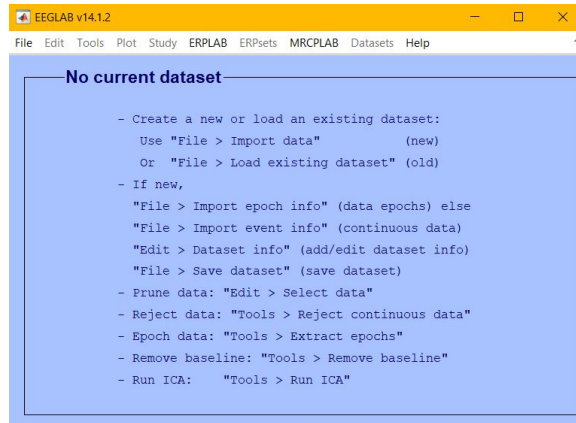


Figure 6.8: EEGLAB Graphical User Interface

data-cleaning on all scalp EEG data and raw EMG data, and extract ERPs time-locked to the acoustic cue (*cf.* section 4). In order to do so, an additional plugin was implemented, called *MRCPLAB*. In order to import data, the user must select *MRCPLAB* → *AutoImport* → *Auto epoch and filter...* (Figure 6.9,A). The plugin allows to import the data coming from all three datasets, by specifying the correct parameters. The user needs to enter, in order (Figure 6.9,B):

- **Sampling frequency:** 0 if read from file, specified if different;
- **Epoch duration:** 0 if taken from cue channel, else specified – for example in the first dataset, when there was no acoustic signal;
- **EMG trace name;**
- **EMG characteristics:** 0 if standard, 1 if impulsive;
- **Cue Channel Name;**
- **EMG Plots:** 0 for no plots, 1 for plotting EMG peaks only, 2 for plotting EMG peaks and cue trace;
- **Spatial Filtering:** 0 for none, 1 for applying Small Laplacian Spatial Filter, 2 for applying Spherical Spline Integral Filter.

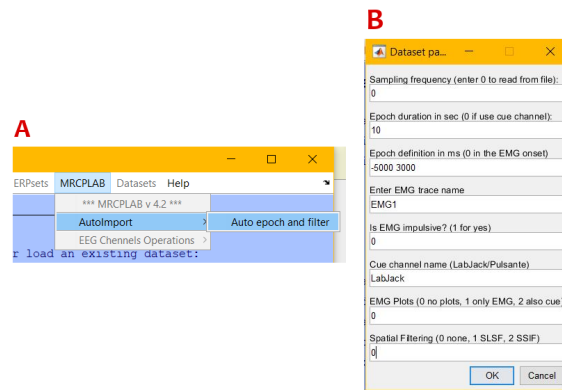


Figure 6.9: MRCPLAB plugin. A) Data importation, B) Parameter setting.

After EEG and EMG data importation, with some simple operations it is possible to display all EEG data and MRCP data (Figure 6.10), alongside the EMG Onset – represented by a red vertical line. By operating on the same interface, it is possible to scroll among epochs and reject invalid data.

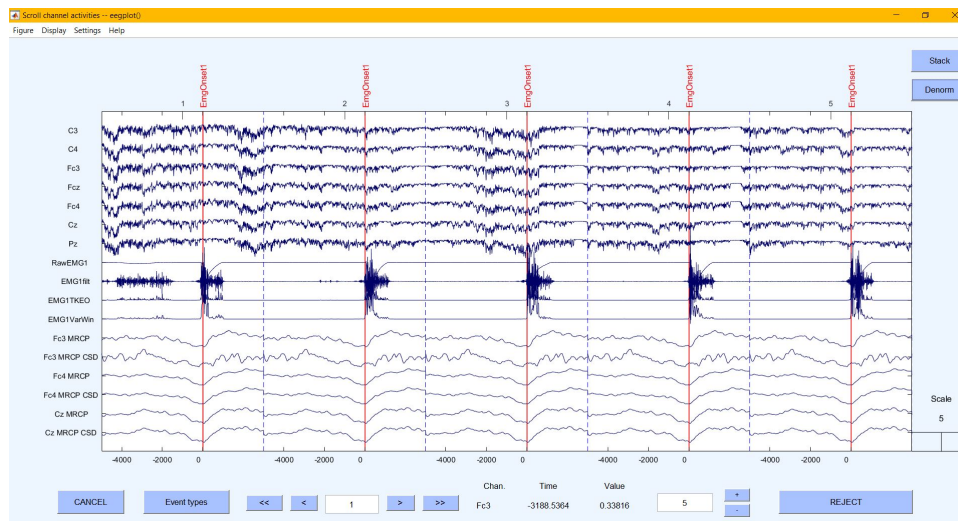


Figure 6.10: Channel data from first dataset acquisition.

# Chapter 7

## Methods

The following sections describe in detail the methods applied for data cleaning, signal processing and further development; they were implemented in MATLAB<sup>®</sup> through self-developed scripts and by the use of the already provided toolboxes. All data were recorded at a sampling frequency of 512 *Hz*. After the importation done through EEGLAB, the electroencephalographic traces alongside with EMG, EOG data and LabJack activations were stored into dedicated structures; this allowed to keep all relevant data in the same variable.

### 7.1 Pre-processing

The collected data featured, in general for all channels, poor SNR. This is due to two main issues: the fact the EEG signal is characterised by really small amplitude – around  $\mu V$  – and that it is often entangled with the noise, making it difficult to separate the two components [14]. In fact, cutting-out all noise components may lead to a significant signal loss, and, on the other hand, retaining most of the signal would inevitably include noise in the data (Figure 7.1). This leads to a trade-off between signal and noise, making it very important to find the correct balance between the two components. For the aim of this project, the choice was to focus on brain activity below 30 *Hz*, since it is more likely to find noise and muscle artifacts at higher frequencies. Moreover, slow-drifts – typically below 0.5 *Hz* – were removed, so as not to affect event-related potential data.

First, it was implemented a **Butterworth Lowpass Filter** of order 11 with the following specifications (Figure 7.2):

- **Cut-off frequency:** 30 *Hz*;
- **Stopband frequency:** 45 *Hz*;
- **Passband ripple:** 3 *dB*;

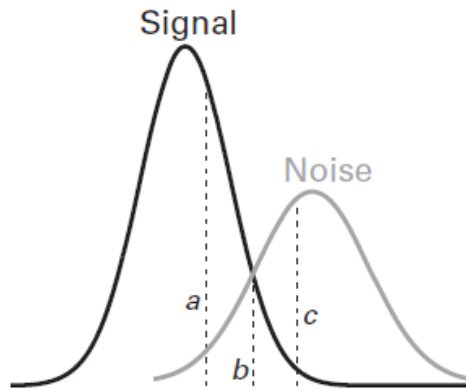


Figure 7.1: Different pre-processing strategies are shown. a) Noise is almost all cut out but a great component of signal is lost; b) trade-off between signal and noise; c) all the signal is maintained but a moderate component of noise is also included [14].

- **Stopband attenuation:** 40 dB.

As regards the slow-drifts removal, a **Butterworth Highpass Filter** of order 3 was implemented (Figure 7.3). The specifications were the following:

- **Cut-off frequency:** 0.5 Hz;
- **Stopband frequency:** 0.1 Hz;
- **Passband ripple:** 3 dB;
- **Stopband attenuation:** 40 dB.

The cut-off and stop-band frequencies were normalized with respect to the Nyquist frequency, calculated as half the sampling frequency. Preprocessing allowed to clean data and go on with data analysis; however, the signal-to-noise ratio didnt improve much, just as expected for a single-trial approach. As mentioned before, the filtering criterion was chosen in order to mantain as much signal as possible; multiple-trials datasets, on the contrary, give the possibility to remove trials that have a huge noise component.

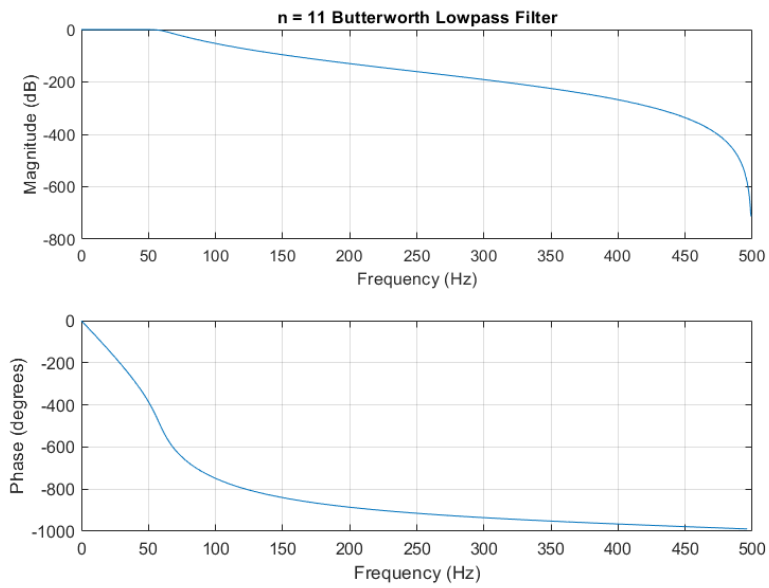


Figure 7.2: Bode Diagram of Butterworth Lowpass filter, order 11.

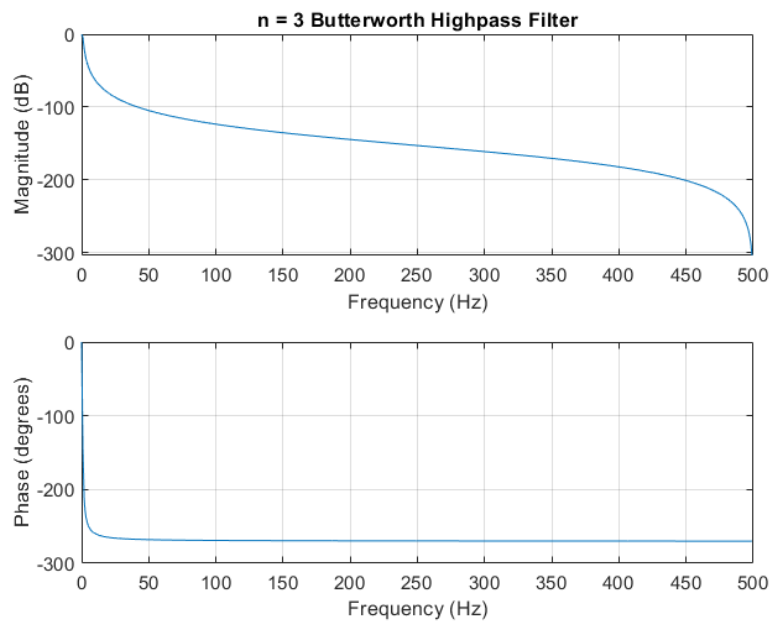


Figure 7.3: Bode Diagram of Butterworth Highpass filter, order 3.

## 7.2 Spatial Filtering

In the view of data filtering, a spatial filtering method was applied: the *Spherical Spline Integral Filter*, also said *surface Laplacian* filter. The surface Laplacian can be described as a spatial bandpass filter: it works by subtracting to each electrode the average activity coming from its surroundings. It was implemented in order to improve topographical localization for the calculation of the MRCP and of the *current scalp density* (CSD) and to reduce topographical noise; the CSD identifies the locations of sources and sinks of electrical currents in the head (Figure 5.2). The surface Laplacian is a reasonable solution since it is reference-independent: it is computed through the second spatial derivative of the potentials; its unit of measurement is  $\mu V/mm^2$ . The best results are obtained on data coming from high-density recording systems (*i.e.* 100 or more scalp electrodes) because, being a filter based on spatial sampling and spatial weighting, the more electrodes are present, the more accurate is the algorithm. In this case, the surface Laplacian was calculated using standard electrode locations (*cf.* section 3.1).

### 7.2.1 Spherical Spline Integral Filter

The Spherical Spline Integral Filter (SSIF) is a method developed to compute the surface Laplacian, presented by Perrin and his research fellows in 1987 [32]; it guarantees fast computational times – about 0.18 s for a 64-channel single-trial EEG [14]. The first step for calculating the SSIF is to compute two matrices,  $\mathbf{G}$  and  $\mathbf{H}$ :

$$G_{ij} = (4\pi)^{-1} \sum_{n=1}^{order} \frac{(2n+1)P_n(\cos dist_{ij})}{(n(n+1))^m} \quad (7.1)$$

$$H_{ij} = (4\pi)^{-1} \sum_{n=1}^{order} \frac{-2(n+1)P_n(\cos dist_{ij})}{(n(n+1))^{m-1}} \quad (7.2)$$

Equations (7.1) and (7.2) represent the electrode-by-electrode weighing matrices;  $i$  and  $j$  are the electrodes,  $m$  is a positive constant value on which depends the smoothness of the results. Values for  $m$  range from 2 to 6<sup>1</sup>; small values return only very high spatial frequencies, whereas large values produce results that contain only very low spatial frequencies.  $P$  is the Legendre polynomial (Figure 7.4), used for spherical coordinate distances and  $n$  is its order. The recommended order is 7 [33], although it depends on the number of electrodes employed – for 64-electrodes systems the order 10 is still accepted. The *cosdist* term represents the cosine distance

---

<sup>1</sup>It can be fixed at 4 for high-density recording systems

among all pairs of electrodes (electrodes locations are normalized to a unit-radius sphere); it is calculated as follows:

$$\text{cosdist}_{ij} = 1 - \frac{(X_i - X_j)^2 + (Y_i - Y_j)^2 + (Z_i - Z_j)^2}{2} \quad (7.3)$$

$\mathbf{G}$  and  $\mathbf{H}$  depend only on the inter-electrode distance; they are used together with EEG data to calculate the surface Laplacian.

$$\text{lap}_i = \sum_{j=1}^{\text{nelec}} C_i H_{ij} \quad (7.4)$$

Equation (7.4) shows the laplacian for the  $i$ -th electrode at one time-point;  $j$  refers to the other electrodes and ranges from 1 to  $\text{nelec}$ , that is 34.  $H_{ij}$  is the element corresponding to  $i$  and  $j$  in the  $\mathbf{H}$  matrix.

$$C_i = d_i - \frac{\sum_{j=1}^{\text{nelec}} d_j}{\sum_{j=1}^{\text{nelec}} G s_j^{-1}} G s^{-1} \quad (7.5)$$

$$d_i = \text{data}_i^{-1} G s \quad (7.6)$$

$$G s = G + \lambda \quad (7.7)$$

In equation (7.7) the smoothing parameter  $\lambda$  is introduced – so,  $G s$  is the smoothed  $\mathbf{G}$  matrix; the recommended value is  $10^{-5}$ , though for high-resolution recording systems smaller values can be used. The  $\mathbf{C}$  matrix contains data; a first spatial derivative through  $\mathbf{G}$  is applied in equation (7.5), in which activity of all electrodes is subtracted from the activity at each electrode. The other spatial derivative is applied in equation (7.4), making the SSIF a second spatial derivative.

## 7.3 Data Filtering

Despite undergoing the pre-processing and spatial filtering steps, other filtering techniques were applied to perform data cleaning and improve further data processing; in fact, all three datasets featured a high percentage of noise. In order to do so, a numerical *Moving Average* (MA) filter was implemented. Moving averages filters are *Finite Impulse Response* (FIR) filters [29].

$$y[n] = b_0 x[n] + b_1 x[n-1] + \dots + b_k x[n-k] \quad (7.8)$$

Equation (7.8) shows the general input-output relation for FIR filters: they compute

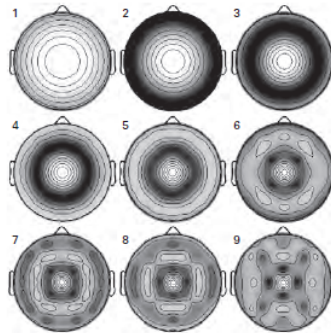


Figure 7.4: Legendre Polynomials related to channel Cz; the first 9 polynomials are shown [14]

a weighted mean of the samples of the input. The transfer function of a general FIR filter is computed as follows:

$$H(z) = b_0 + b_1z^{-1} + \dots + b_kz^{-k} \quad (7.9)$$

The expression in equation (7.9) demonstrates that a FIR filter is always stable, as the poles are located in the origin – inside the *unit circle*. The selected *time span* parameter for the implemented MA filter was 5.

## 7.4 EMG onset detection

EMG onset detection is a really important step as it determines the outcome of data processing. The ideal situation would be having an impulsive signal – for example, a sequence of isoelectric line and action potential – so that the detection could be based on setting a threshold on the EMG voltage value. However, in real experimental settings this condition is hard to reach; in fact, the action potentials are mixed with noise. EMG onset detection is a really important step as it determines the outcome of data processing. The ideal situation would be having an impulsive signal – for example, a sequence of isoelectric line and action potential – so that the detection could be based on setting a threshold on the EMG voltage value. However, in real experimental settings this condition is hard to reach; in fact, the action potentials are mixed with noise. In order to find the time instant corresponding to muscle activation, the **Teager-Kaiser Energy Operator** (TKEO) was implemented. This method was developed to allow better EMG detection in surface EMG recordings [27]; it relies on the following parameter:

$$\Psi_d x[n] = A^2 \sin^2[\omega_0(n)] \quad (7.10)$$

Equation (7.10) introduces the TKE operator ( $\Psi$ ), which is related to the amplitude and frequency ( $A, \omega_0$ ) of the generated action potential. After TKEO implementation, the EMG onset is identified by setting a threshold.

## 7.5 Epochs

Single-trial EEG data are stored in 2D matrices organized so that the rows contain electrodes data. To the purpose of this study, each channel trace must be divided into segments time-locked to a particular event – that is, the EMG onset (*cf.* section 6.1). After epoching, the time-domain channel data were stored into 3D matrices containing electrodes, time and trials. The epochs must be at least as long as the duration of the trial; choosing the right window affects significantly the outcomes of signal processing (Figure 7.5). The obtained epochs contained 1024 samples, resulting in a total duration of 2 s. To cut the signal into epochs, two different approaches were followed, depending on the type of acquisition.

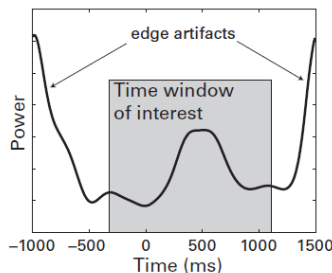


Figure 7.5: Signal epoching. Choosing the correct window allows, in this case, to reject edge artifacts [14]

### Creating epochs: first dataset

During the first dataset acquisition there was no acoustic signal determining when to perform the movement, so each trace was cut into 10 s segments that ended with the EMG onset. With this method, each single-trial trace was divided into 40 epochs.

### Creating epochs: second and third datasets

During the second and third dataset acquisitions, the subject was instructed to follow the time pattern marked by the acoustic signal. In this case, the epochs depend both on the occurrence of the acoustic cue and on the EMG onset; thus, the audio sound marked the beginning of each epoch, that ended with the movement realization. Also in this case the generated epochs were 40.

### 7.5.1 Averaging Technique

After dividing the signal into epochs, the aim is to extract the MRCPs that will be used in further data analysis. This was carried out by means of the averaging technique; although it is an advanced method that is usually employed for denoising. It can be applied only when the signal of interest can be considered as a repetition in time of an identical waveform due to stimulation or physiological responses.

$$MRCP_j = \frac{1}{N} \sum_{i=1}^N x_i(t) \quad (7.11)$$

The motor related cortical potentials are extracted as shown in equation (7.11), by taking the mean of all epochs;  $j$  represents the electrodes,  $N$  is the number of calculated epochs (40),  $x_i(t)$  is the  $i$ -th epoch. With this technique, the MRCPs related to each channel were successfully extracted (Figure 7.6). The grand-average cortical potential is computed by taking the mean of all MRCP obtained in equation (7.11).

$$GA = \frac{1}{N} \sum_{i=1}^N MRCP_i \quad (7.12)$$

In equation (7.12),  $N$  represents the number of channels; the grand-average MRCP is shown in Figure 7.7: it is possible to observe the negative deflection occurring 1.5 s before movement onset, related to the beginning and end of the readiness potential.

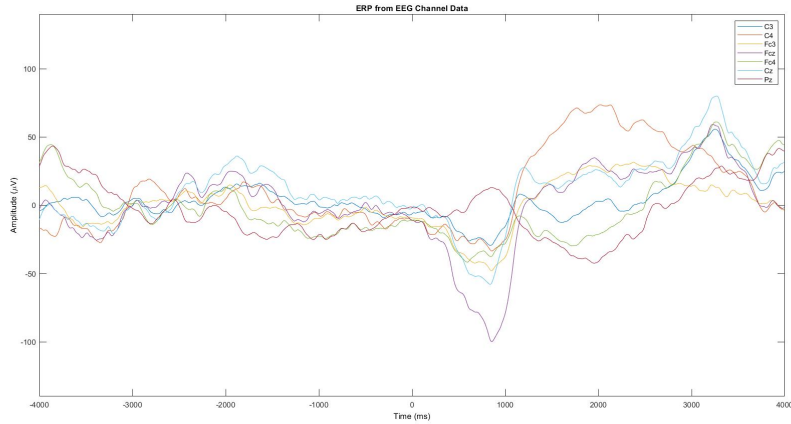


Figure 7.6: Motor Related Cortical Potentials extracted from subject #3, dataset #1.

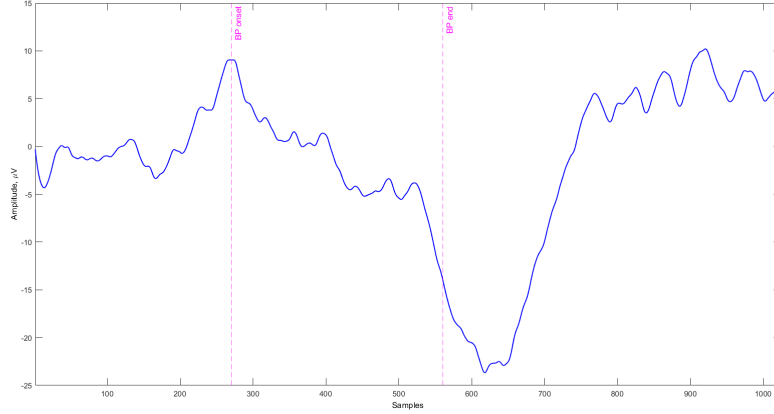


Figure 7.7: Grand-average plot of MRCPs; the readiness potential starts about 1.5 s before movement actualization and the negative deflection stops 0.5 s before (purple dotted lines).

## 7.6 Spectral Density Estimation

The *power spectral density* (PSD) was computed in order to locate the EEG trials and relative MRCP into specific frequency bands. It was implemented by means of a classical approach and applied to data contained in the first dataset, because they featured better quality MRCPs. The chosen technique was the **method of Welch**, that aims at reducing the variance of the estimate by averaging more periodograms. The *periodogram* and its variance are defined in equations (7.13) and (7.14) respectively:

$$\hat{P}_x(f) = \frac{1}{N} \left| \sum_{n=0}^{N-1} x[n] e^{-2\pi f n} \right|^2 \quad (7.13)$$

$$\text{var}[\hat{P}_x^2(f)] = \hat{P}_x^2(f) \left[ 1 + \left( \frac{\sin 2\pi f N}{N \sin 2\pi f} \right)^2 \right] \quad (7.14)$$

After computing PSD of EEG data and MRCPs, the conventional bandpower percentages were estimated, thus identifying the frequency components that characterise the mother-signal and cortical potentials. The steps are described in algorithm 1.

---

### Algorithm 1 Bandpower estimation

---

- 1: Compute PSD of EEG data;
  - 2: Collocate PSD in conventional frequency bands;
  - 3: Divide band-PSD by total PSD.
-

### 7.6.1 EEG trials

The PSD of EEG data was computed so as to perform a pre-screening task. EEG recorded traces contain about 70 thousand samples; in order to enhance computational velocity only 15 thousand samples were taken into account – enough for the purpose said above. The chosen parameters are the following:

- **Sampling frequency:** 512  $Hz$ ;
- **Theoretical resolution:** 0.512  $Hz$ ;
- **NFFT:** 1000;
- **Window:** Hamming, 1000 samples (7.8);
- **Overlapping:** 500 samples.

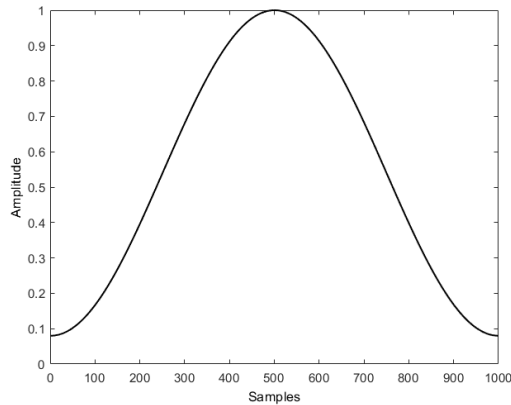


Figure 7.8: Hamming window used for windowing EEG trial data.

### 7.6.2 MRCP

The motor related cortical potential is 1024 *samples* long. The parameters for PSD estimation were set as follows:

- **Sampling frequency:** 512  $Hz$ ;
- **Theoretical resolution:** 5.12  $Hz$ ;
- **NFFT:** 100;
- **Window:** Hamming, 100 samples (7.8);
- **Overlapping:** 50 samples.

## 7.7 Matched Filter

The aim of this study was to find patterns of volitional movement and differentiate them from semivoluntary – or *voluntary-induced* activity patterns, in order to find evidence of the effect of habit during complex tasks; this was carried out by implementing a matched filter. This technique was applied to data coming from the second and third dataset acquisition, as they involved both voluntary and semivoluntary task recordings. Only channel data regarding the frontal lobe was taken into account. The matched filter is a linear filter that relies on a convolution operation between a signal and a given impulse response; it is obtained by correlating a known pattern with an unknown signal [42].

$$MF_i = \int_{-\infty}^{\infty} h(t - \tau)x(\tau) \quad (7.15)$$

Equation (7.15) describes the matched-filter relation for a continuous-time system;  $x(\tau)$  is the unknown signal – in our case the EEG channel data, and  $h(t - \tau)$  is the impulse response that is represented by the MRCPs. The motor-related cortical potentials extracted from single-trial EEG data recorded during the voluntary task were used as impulse response; this choice was made because the presence of MRCPs in healthy subjects prior to volitional movement actuation is certain. The unknown signal was represented by the channel data collected during the semivoluntary task; in fact, although the processing was performed only on healthy subjects' EEG traces, we are not sure about the brain activation patterns that occur in the PMC and pre-motor cortex. The event-related potentials were expressed in terms of numerator coefficients; the denominator coefficient was 1, so the implemented filter is an *all-zero* FIR filter (*cf.* equation (7.8)) with linear phase. The detection threshold was set to 0.9. The implemented convolution is channel-dependent, meaning that the MRCP corresponding to channel '1' is convoluted with the EEG trace of the same channel. The output of the matched filter should be a signal made of a sequence of peaks (Figure 7.9), where each peak identifies the time-point where the readiness potential matches the single-trial EEG data. If the brain voluntary pattern is attenuated, then it is expected to find fewer or lower amplitude peaks (Figure 7.10).

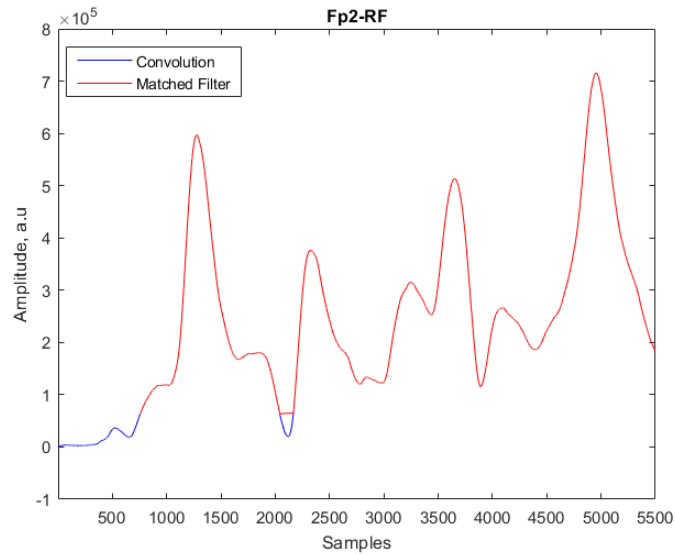


Figure 7.9: Matched filter output related to subject #2, channel FP2. The first 10 s of recording are shown; the samples that meet the set threshold are pictured in red. The definite peaks correspond to volitional activity.

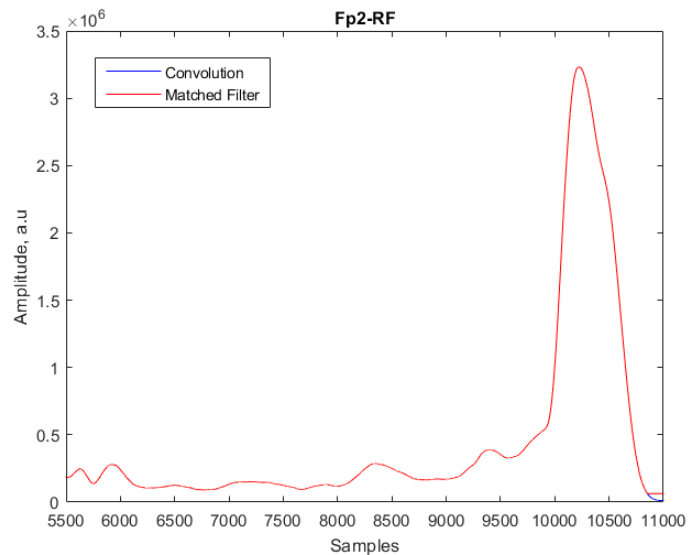


Figure 7.10: Matched filter output related to subject #2, channel FP2. Seconds 10 to 21 are shown. There is only one definite peak.

## 7.8 Data analysis

The last step consisted in statistical considerations on the movement-related cortical potentials, performed in order to give a quantitative interpretation of their meaning. Two different approaches were followed, depending on the dataset involved.

### 7.8.1 First dataset

During the first dataset acquisition, the EEG montage included 6 scalp electrodes covering the PMC and SMA and one electrode positioned on the somatosensory cortex (*cf.* section 6.1.1). As mentioned in section 5.1, according to some studies the readiness potential is lateralized; the aim is to find evidence of this consideration. To the purpose of this analysis, the electrodes positioned over the cerebral longitudinal fissure are taken as reference. Then, for each subject, the correlation coefficient is computed between laterally-positioned electrodes and the reference, and between contralateral electrodes as a measure of their linear dependence.

$$\rho_{A,B} = \frac{1}{N-1} \sum_{i=1}^N \left( \frac{A_i - \mu_A}{\sigma_A} \right) * \left( \frac{B_i - \mu_B}{\sigma_B} \right) \quad (7.16)$$

Equation (7.16) describes the Pearson correlation coefficient for two variables (A and B),  $\mu$  and  $\sigma$  are the mean value and standard variation of the two variables and N is the number of observations – in our case, the subjects. Thus, the Pearson coefficient is computed for all subjects for the following MRCs (the Pz electrode is discarded since it is not of interest for the analysis):

1. **FC3 - FCz;**
2. **FC4 - FCz;**
3. **C3 - Cz;**
4. **C4 - Cz;**
5. **FC3 - FC4;**
6. **C3 - C4.**

Then, for each condition, the mean, standard deviation and skewness are computed over all subjects. The steps are described in algorithm 2.

---

**Algorithm 2** Pearson Coefficient, Lateralized Readiness Potential

---

- 1: Select subject;
  - 2: Select channel;
  - 3: Compute MRCP;
  - 4: Repeat 3 for all channels;
  - 5: Repeat 1-3 for all subjects;
  - 6: Select condition;
  - 7: Calculate Pearson coefficient of the MRCPs regarding the chosen condition;
  - 8: Repeat 7 until all conditions are covered;
  - 9: Repeat 6-8 for all subjects;
  - 10: For each condition, calculate mean, STD and skewness over all subjects.
- 

### 7.8.2 Second and third datasets

The second and third datasets were recorded with a high-density system consisting of 34 scalp electrodes. The electrodes covered all four brain lobes, thus registering motor-related activity, visual and proprioceptive information simultaneously. The aim is to investigate the correspondence between the brain patterns generated in the voluntary and semivoluntary tasks, respectively. For each subject, the Pearson coefficient is calculated between the voluntary and semivoluntary task cortical potentials, and then the mean is taken over all subjects. The steps are described in algorithm 3.

---

**Algorithm 3** Pearson Coefficient, Voluntary vs Semivoluntary task

---

- 1: Select subject;
  - 2: Select channel;
  - 3: Compute MRCP for the voluntary and semivoluntary task;
  - 4: Calculate Pearson coefficient of the obtained voluntary and semivoluntary cortical potentials;
  - 5: Repeat 3 for all channels;
  - 6: Repeat 1-4 for all subjects;
  - 7: For each channel, calculate the mean Pearson coefficient over all subjects.
-

# Chapter 8

## Results

This section contains the results and comments of the methods applied for EEG data processing and analysis; they are organised following the outline introduced in chapter 7.

### 8.1 Pre-processing and filtering results

As said in section 7.1, the imported single-trial EEG data undergo pre-processing steps and spatial filtering; it is possible to see the results through a feature of EEGLAB, that displays all channel data and allows to navigate through the epochs (Figure 8.1). Despite the applied methods, electroencephalographic data – especially in datasets 2 and 3 – proves to be still affected by some recording artefacts. This may be due to the fact that, although the skin underwent proper preparation, the scalp impedance is still too high to guarantee a good SNR. In the view of future experimental sessions, dedicated maintenance work was performed on the amplifier and its connected hardware; the headcap electrodes and Galileo amplifier’s inputs impedance were controlled by means of a multimeter and adjustments were made when needed. 23 out of 69 trials (about 33%) belonging to datasets 2 and 3 needed to be discarded because of LabJack signal failure: it was impossible to separate the train of voltage impulses from background noise; this issue was fixed during maintenance by working on the photocoupler circuit connected to the DAQ board. Spatial filtering improved data quality by reducing topographical noise and allowed to obtain the CSD, identifying the electrical activity sources of the cerebral cortex. The result is shown in Figure 8.2 and in Figure 5.2, in chapter 5 – where the Bereitschaftspotential was introduced.

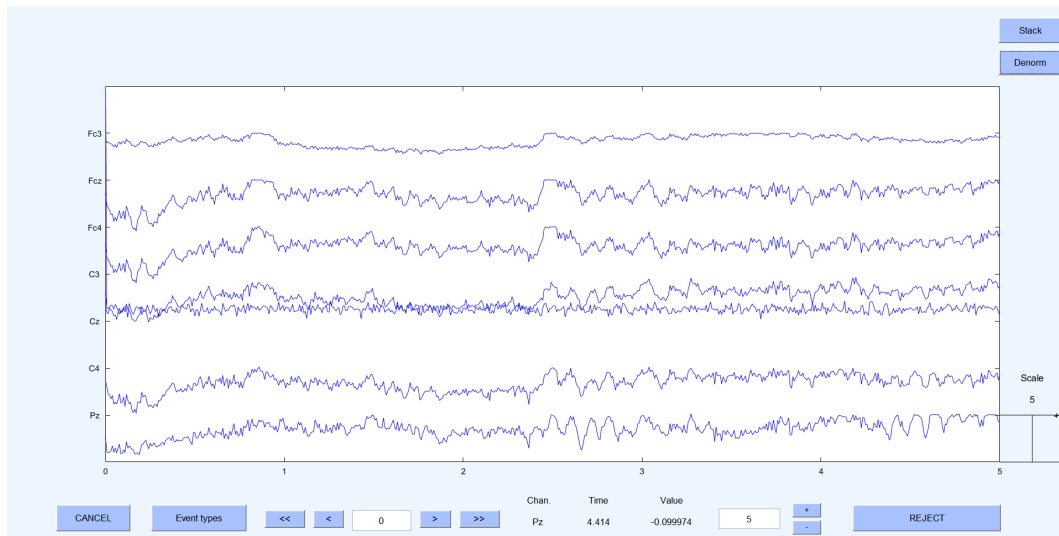


Figure 8.1: EEG channel data of subject 1, first dataset (voluntary task). Data from the 7 scalp electrodes is shown.

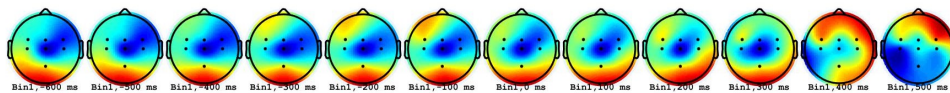


Figure 8.2: CSD, the output of spatial filtering. The figure shows the electrical patterns from 600 *ms* prior to movement actualization to 500 *ms* after movement.

## 8.2 EMG Processing results

Section 6.1.2 explained how from the second dataset acquisition on, the motor action potential was elicited by an acoustic signal heard by the subject. The signal is converted into a voltage one by means of an optocoupler circuit and the LaJack DAQ board, that digitalizes the signal into a square wave of amplitude  $8 \mu V$  (Figure 8.3); The EMG onset is to be found after the square-wave ramp. By applying the methods described in section 7.4, EMG raw data is processed into an impulsive signal, in which the movement onset is easily identified, as Figure 8.4 shows.

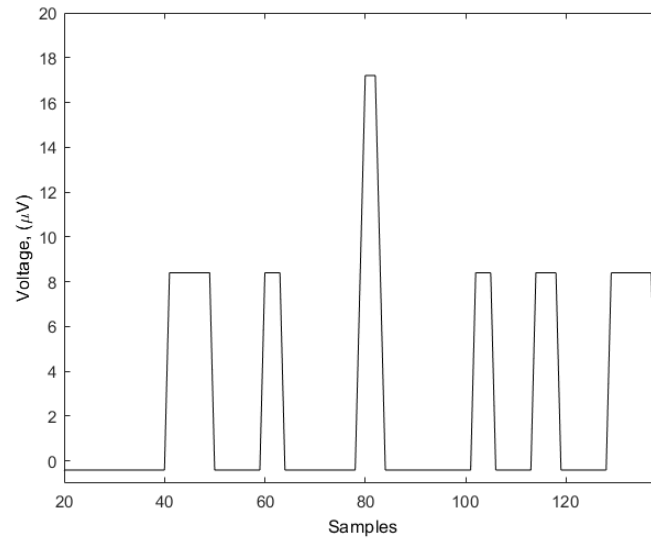


Figure 8.3: DAQ output signal, displayed as a sequence of square waves that indicate the occurrence of the acoustic cue.

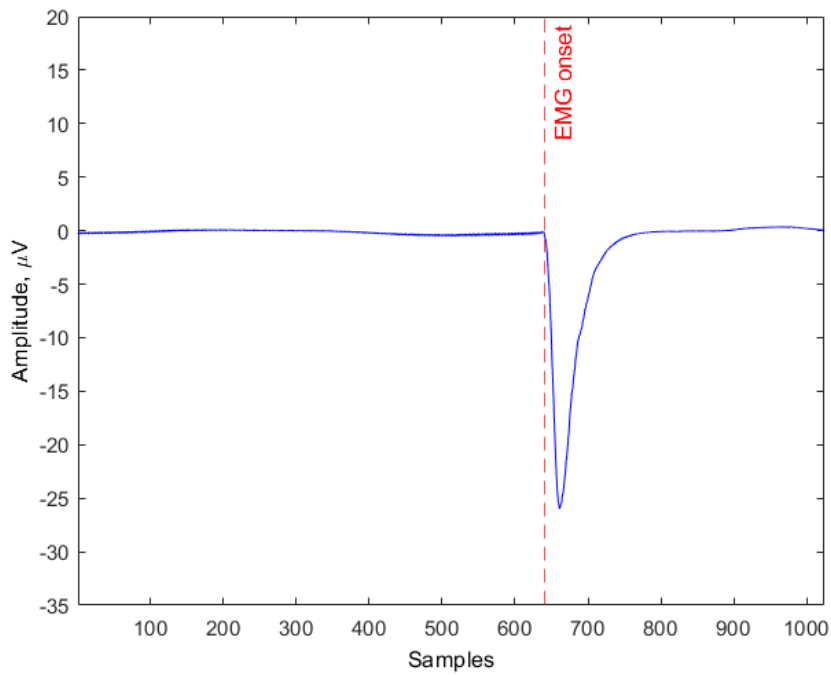


Figure 8.4: Processed EMG data, the waveform is definite and the red dashed line represents the onset.

### 8.3 Averaging results

As said in section 7.5, the epochs are created according to the time instant of the EMG onset. Averaging across epochs is a useful way to excerpt MRCPs from EEG channel data without losing significant signal components. The result obtained from dataset 1 is shown in Figure 8.5; the cortical potentials range from  $-40 \mu V$  to  $25 \mu V$  and are synchronised in all channels. The negative deflection starts about 2 seconds before movement onset – time 0 s in the plot; a similar outcome – but relative to another subject – is shown in chapter 7, Figure 7.6. In order to better understand the trend of this brain activation pattern, the Grand-Average plot is obtained as the plain average of channel MRCPs (Figure 8.6). The amplitude range is  $35 \mu V$ .

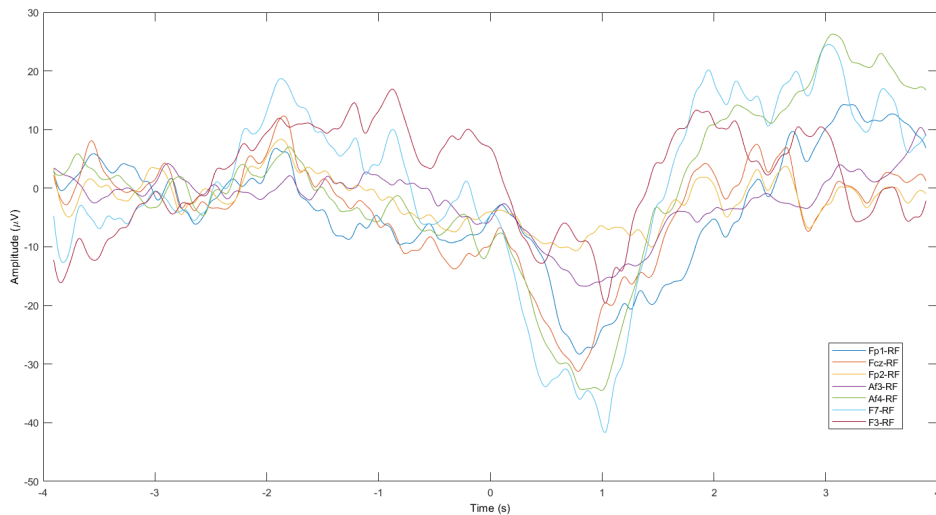


Figure 8.5: MRCPs obtained from averaging scalp EEG data of subject 5; 7 scalp channels are shown.

### 8.4 Spectral Density Estimation results

Offline spectral density estimation is carried on for two reasons: firstly, to check that the subject is awake during the task and, later, to identify specific frequency bands that characterise the event-related potentials. The methods and chosen parameters are described in section 7.6.

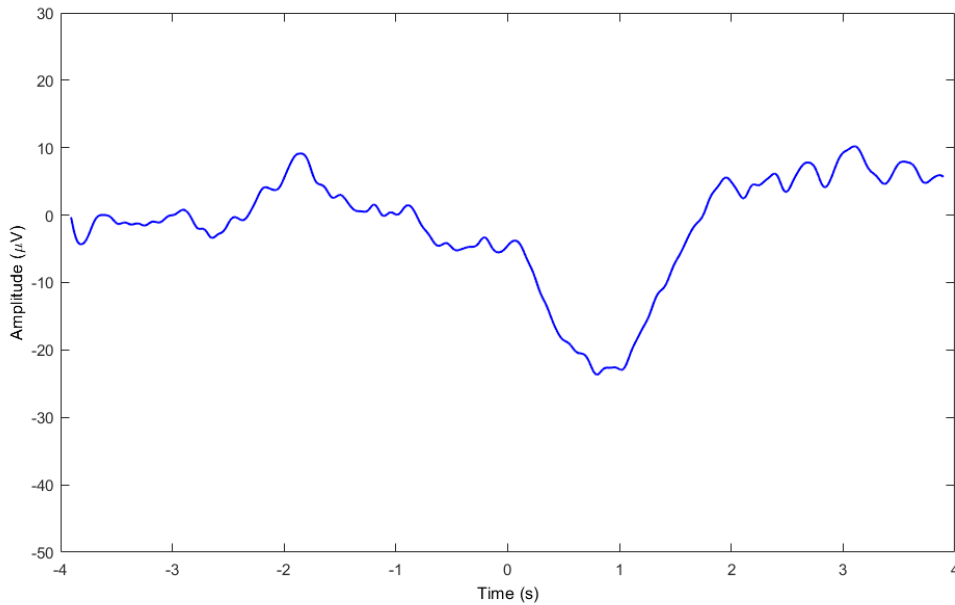


Figure 8.6: Grand-Average Plot, subject 5

### 8.4.1 Bandpower estimation: EEG Data

This section contains the results of periodogram estimation performed on healthy subjects recordings, since injured subject data is confidential and Health Etical Committee approval is stil pending. The selected conventional bandwidths are the following:

- **Delta band:**  $0.5 - 3.5 \text{ Hz}$ ;
- **Theta band:**  $3.5 - 7 \text{ Hz}$ ;
- **Alpha band:**  $7 - 14 \text{ Hz}$ ;
- **Beta band:**  $> 14 \text{ Hz}$ .

This method is applied to all subjects and at the end the mean is taken. Table 8.1 shows the results for the most significant electrodes; each row corresponds to a channel and the columns correspond to the frequency bands. As expected, the majority of power belongs to the  $\beta$ -rhythm, found in the frontal lobe of the healthy adult during task performance;  $\alpha$ -band is suppressed since the subject lies in a state of alertness. Also  $\theta$ -band and  $\delta$ -band feature small power percentage, as expected. [29]. The power percentage is slightly larger in the left-located electrodes.

	$\beta$	$\alpha$	$\theta$	$\delta$
<b>C3</b>	50 %	0.45 %	1.39 %	17.39 %
<b>C4</b>	46.80 %	0.42 %	1.30 %	18.09 %
<b>Cz</b>	48.18 %	0.43 %	1.33 %	17.81 %
<b>FC3</b>	50.72 %	0.45 %	1.40 %	17.28 %
<b>FC4</b>	32.17 %	0.29 %	0.89 %	17.81 %
<b>FCz</b>	48.35 %	0.43 %	1.34 %	17.28 %
<b>Pz</b>	43.34 %	0.39 %	1.20 %	18.76 %

Table 8.1: Bandpower percentage results of healthy subjects channel data.

### 8.4.2 Bandpower estimation: MRCP Data

The method of Welch, with the parameters described in 7.6 is applied to MRCPs in order to be able to find their location in the frequency spectrum. Unexpectedly, this kind of event-related potential has a huge component in the low-frequency area. Thus, instead of using the conventional EEG rhythm division, four bands are defined:

- **Very Low Frequency (VLF):**  $0.1 - 3 \text{ Hz}$ ;
- **Low Frequency (LF):**  $3 - 8 \text{ Hz}$ ;
- **Medium-low Frequency (MLF):**  $8 - 15 \text{ Hz}$ ;
- **High Frequency (HF):**  $> 15 \text{ Hz}$ .

	<b>VLF</b>	<b>LF</b>	<b>MLF</b>	<b>HF</b>
<b>C3</b>	34 %	1.86 %	1.60 %	0.16 %
<b>C4</b>	31.92 %	7.67 %	3.90 %	0.40 %
<b>Cz</b>	43.66 %	3.45 %	2.06 %	0.12 %
<b>FC3</b>	81.40 %	10.33 %	3.89 %	0.39 %
<b>FC4</b>	62.57 %	1.58 %	1.35 %	0.23 %
<b>FCz</b>	62.38 %	3.06 %	1.15 %	0.08 %
<b>Pz</b>	71.28 %	1.40 %	0.67 %	0.16 %

Table 8.2: Bandpower estimation of Motor Related Cortical Potentials

As table 8.2 shows, the higher power percentage is found in the VLF band. This outcome could be useful for future studies, suggesting that, by setting the proper

interval boundaries, cortical potentials can be investigated through frequency-based methods.

## 8.5 Matched Filter results

The motor-related cortical potentials related to the voluntary task are convoluted with the single-trial EEG data recorded during the semivoluntary task; a linear matched filter is created, with set matching threshold 0.9. The aim is to investigate the nature of the semivoluntary cerebral pattern. The procedure is described in section 7.7. Here, only results related to channels located in the PMC, pre-motor area and supplementary motor area will be discussed.

### 8.5.1 General outcome

The best results are obtained in the FP channels: FC and AF channels are very noisy; this is due, especially for the latter, to their location over the frontal lobe, that is responsible for concentration and planning but also for emotional expression, orientation and judgement. The general trend shows that, in the first epochs of the trial, there is at least one matching peak per epoch, suggesting that, at least during the first 2 *min*, the semivoluntary task presents high correlation with the completely voluntary one. As Figure 8.7 shows, mid-trial epochs (from 10 to 22) do not display definite peaks. During the final part of the task (epochs 23-40), high peaks are present again. This suggests the effect of habit during complex task performance; that is attenuated when the subject becomes aware again. The same holds for Figure 8.8. As regards AF channels (Figure 8.9, 8.10), which are located in the pre-frontal cortex, the matched filter output recalls a white noise pattern. As mentioned before, although their coverage accounts for complex task management, they also process emotional information and manage social interaction patterns, thus making it difficult to recognize specific motor brain-patterns – especially when the amplitude is really low, as in the case of MRCPs. The same outcome is obtained in FC channels, as expected, since they are affected also by the electrical eye activity (they are located above the frontal eye field cortex area). An example is shown in Figure 8.11. The effect of habit and the uncorrelation between voluntary and semivoluntary task is better seen in Figure 8.12, that shows the envelope of the matched filter output. In fact, it features only one definite peak at the beginning of the task; throughout the rest of the trial the peaks are smaller in amplitude, suggesting that the primary motor cortex underwent adjustment in order to stick to the semivoluntary task.

## 8.5. MATCHED FILTER RESULTS

---

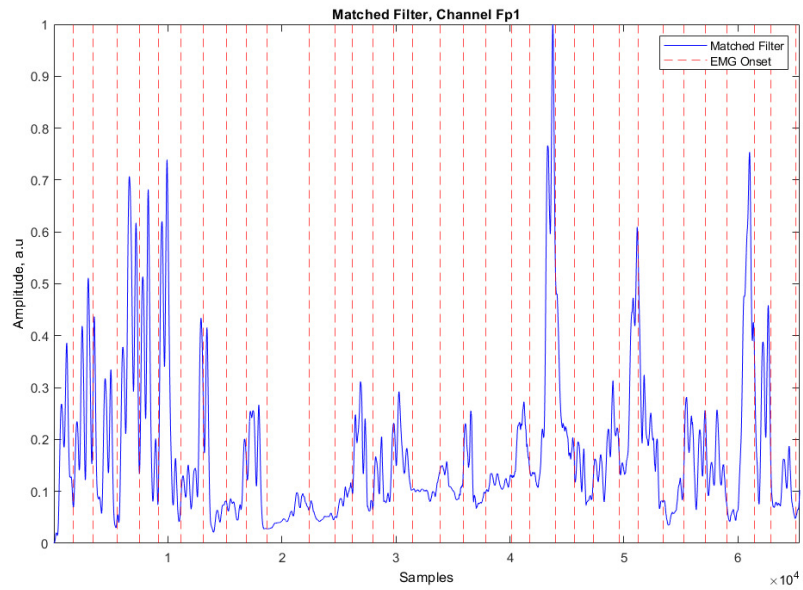


Figure 8.7: Matched Filter output: channel FP1, subject 1. The red dashed lines represent EMG onset and define the epochs.

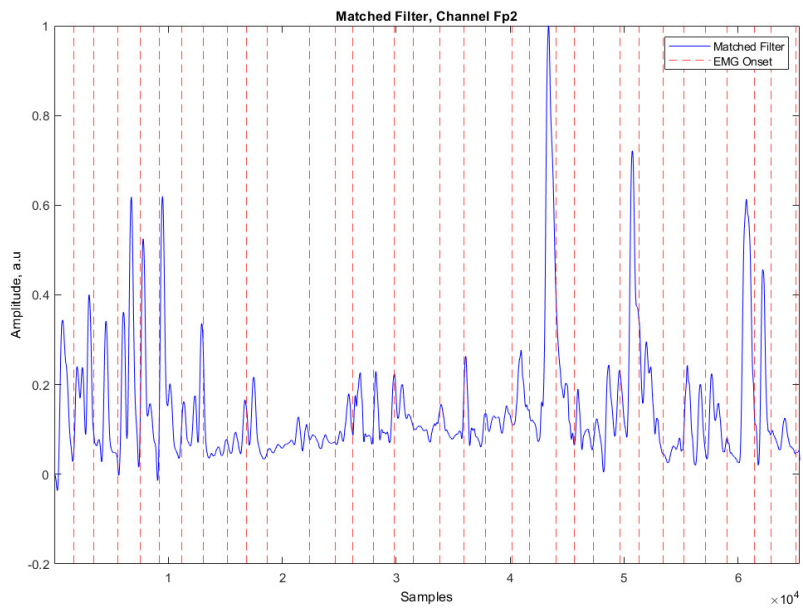


Figure 8.8: Matched Filter output: channel FP2, subject 1. The red dashed lines represent EMG onset and define the epochs.

## 8.5. MATCHED FILTER RESULTS

---

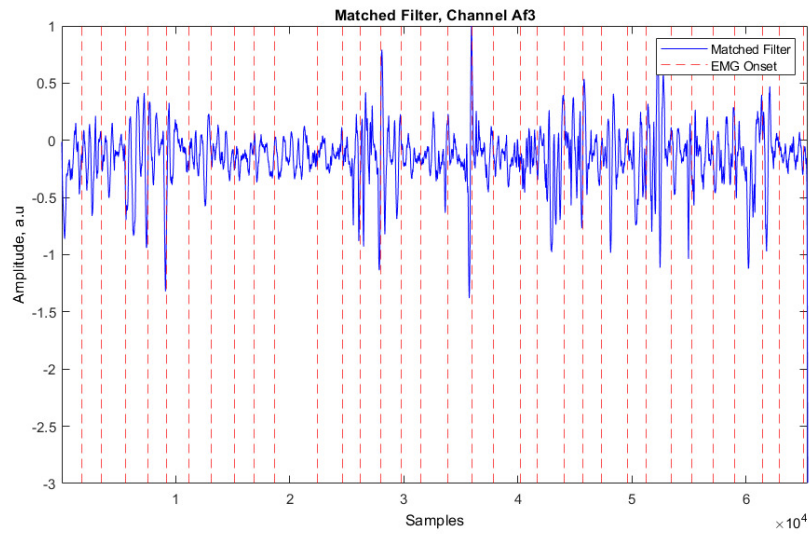


Figure 8.9: Matched Filter output: channel AF3, subject 1. The red dashed lines represent EMG onset and define the epochs.

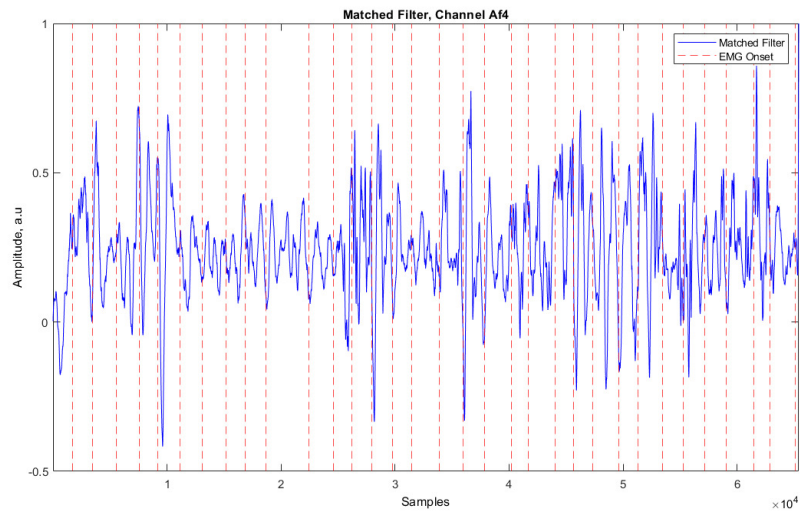


Figure 8.10: Matched Filter output: channel AF4, subject 1. The red dashed lines represent EMG onset and define the epochs.

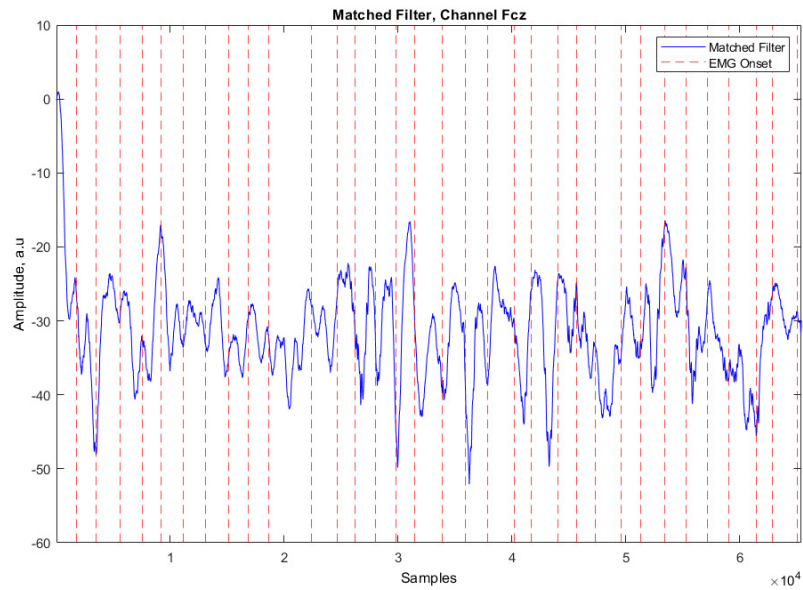


Figure 8.11: Matched Filter output: channel FCz, subject 1. The red dashed lines represent EMG onset and define the epochs.

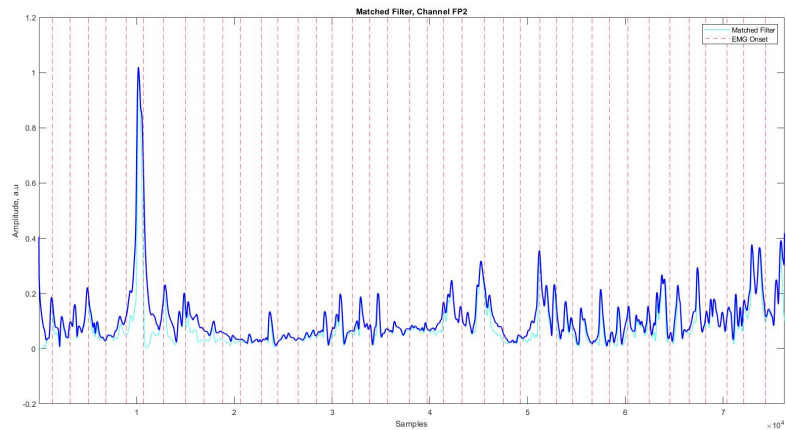


Figure 8.12: Matched Filter output: channel FP2, subject 5. The red dashed lines represent EMG onset and define the epochs, the blue line is the matched filter envelope.

## 8.5.2 Epochs details

With respect to the data presented in the previous section, the details of the epochs are shown here for FC1 and FP1 channels of subject 1. The majority of early epochs present a matching peak in the range of 2 s prior EMG onset; the same pattern is found in some epochs towards the end of the trial. The epochs related to the middle part of the task do not show significant matching peaks. As shown in Figure 8.19, 8.18, epochs 1 and 7 in channel FP1 present more than one peak; to the purpose of this study only the earliest peak – going backwards from EMG onset – is considered. Figure 8.21 shows epoch 25 of the same channel; it is possible to observe two definite peaks, which are, however, discarded due to the occurrence time. In conclusion, secondary peaks cannot be properly interpreted due to the complex nature of brain electrical activity; in fact, some functional areas in the cerebral cortex are appointed the management of multiple – and sometimes diversified – activities.

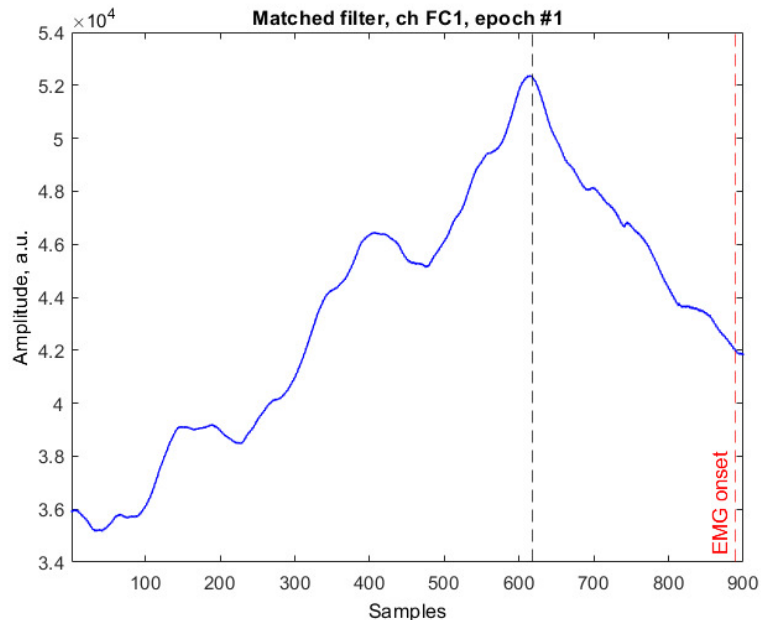


Figure 8.13: Detail of epoch 1, channel FC1, subject 1. A significant peak is observed about 0.6 s before movement onset.

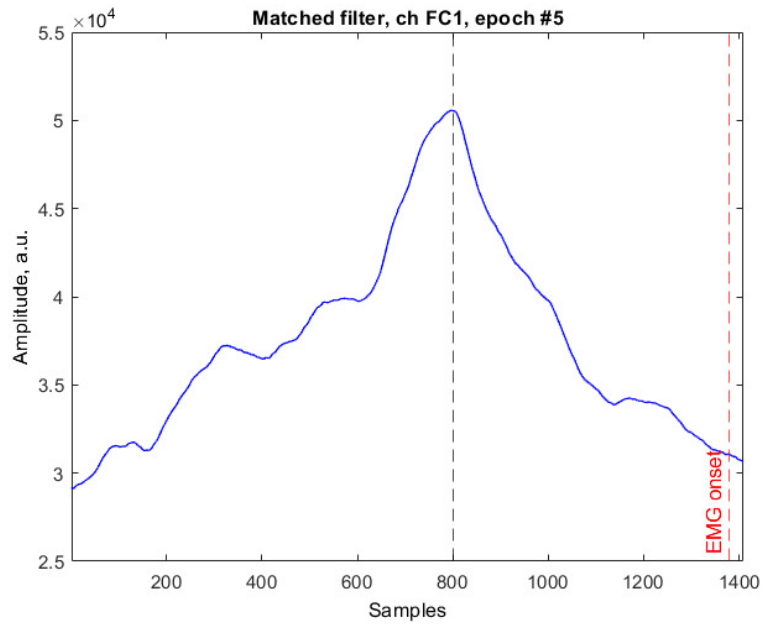


Figure 8.14: Detail of epoch 5, channel FC1, subject 1. A significant peak is observed 1.2 s before movement onset.

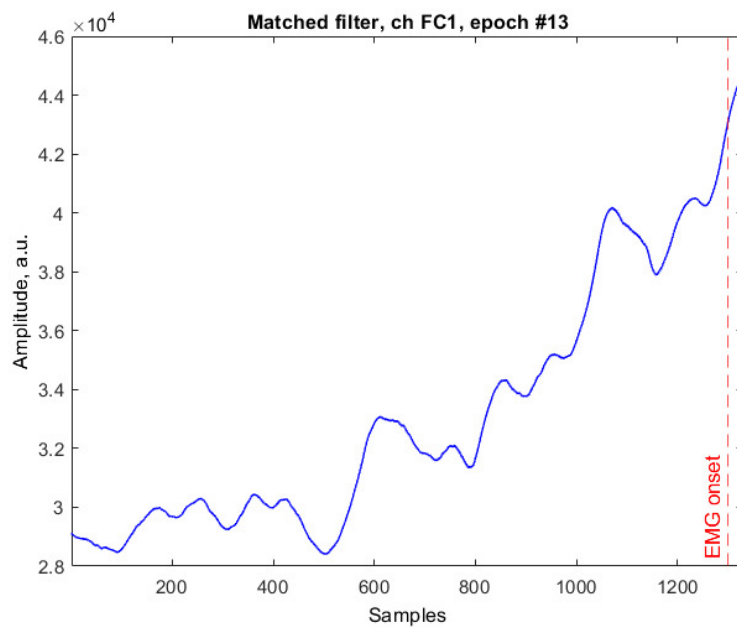


Figure 8.15: Detail of epoch 13, channel FC1, subject 1. No significant peaks occur in a time-window of 2 s prior to EMG onset.

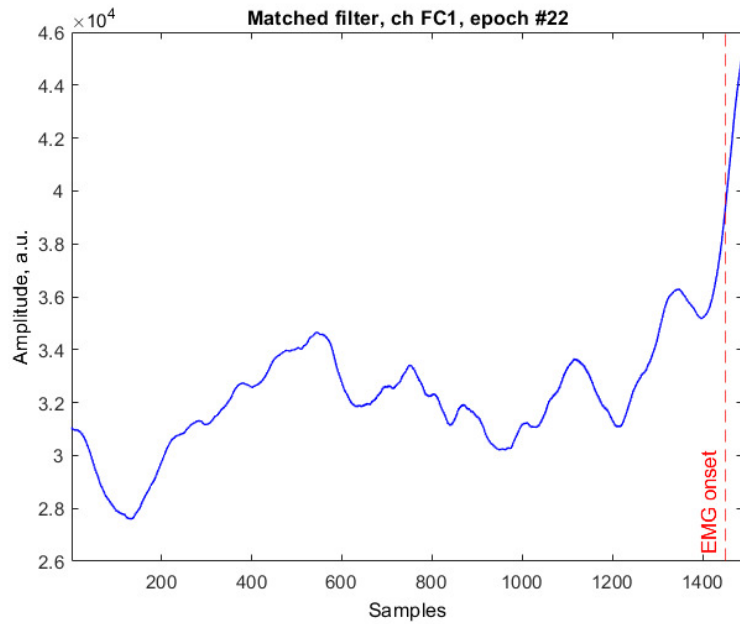


Figure 8.16: Detail of epoch 22, channel FC1, subject 1. No significant peaks occur in a time-window of 2 s prior to EMG onset.

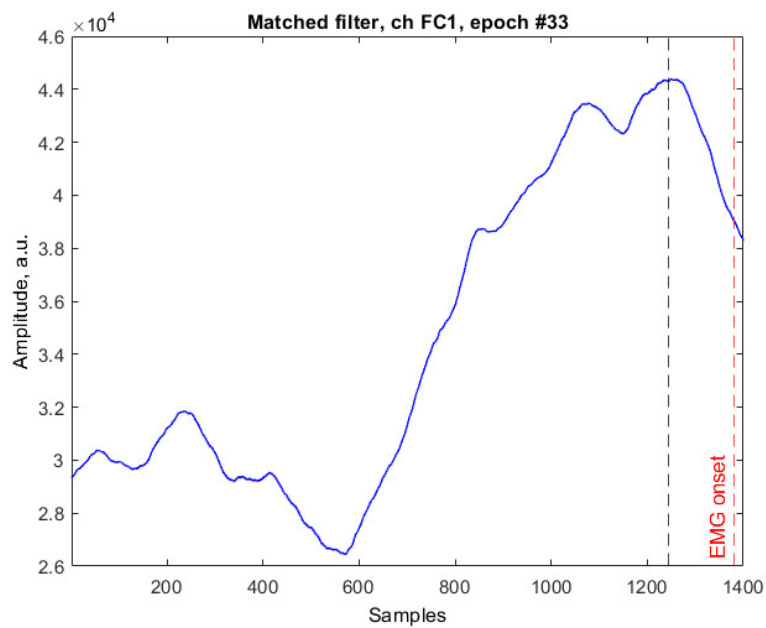


Figure 8.17: Detail of epoch 33, channel FC1, subject 1. A significant peak is observed 0.5 s before movement onset.

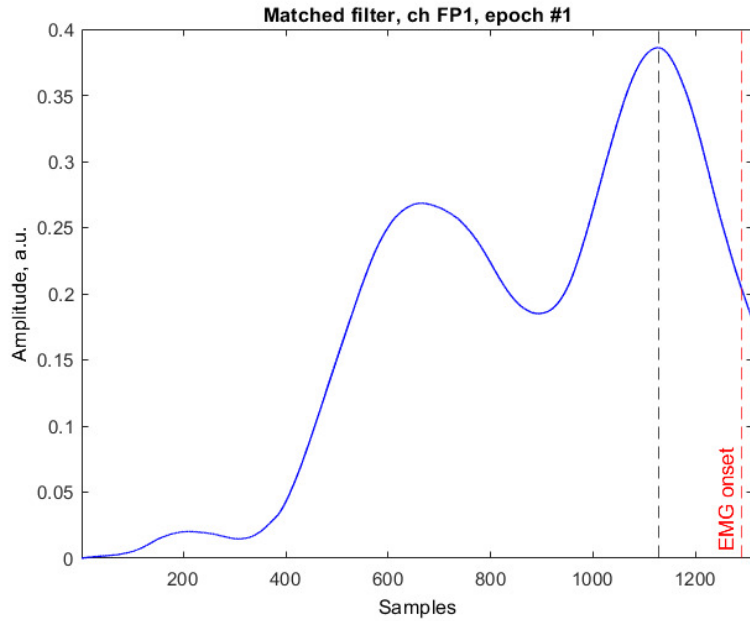


Figure 8.18: Detail of epoch 1, channel FP1, subject 1. A significant peak is observed 0.5 s before movement onset.

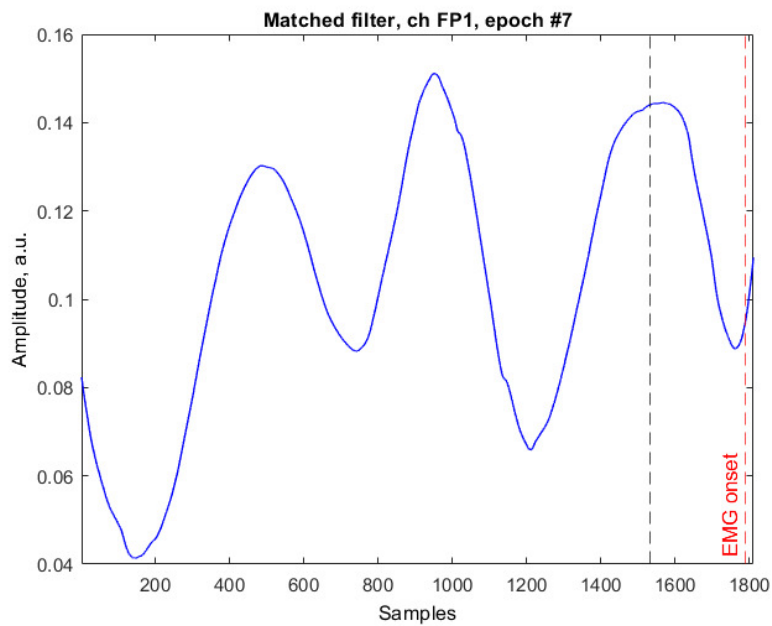


Figure 8.19: Detail of epoch 7, channel FP1, subject 1. A significant peak is observed 0.5 s before movement onset.

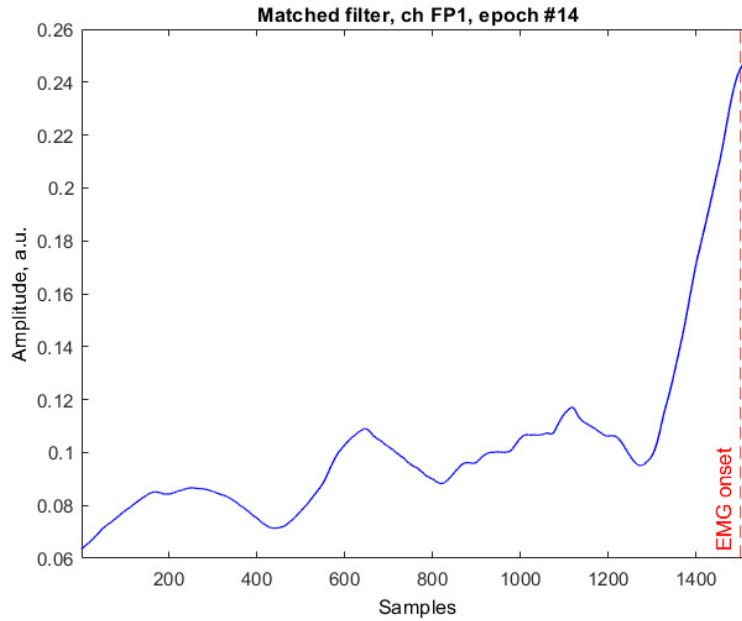


Figure 8.20: Detail of epoch 14, channel FP1, subject 1. No significant peaks occur in a time-window of 2 s prior to EMG onset.

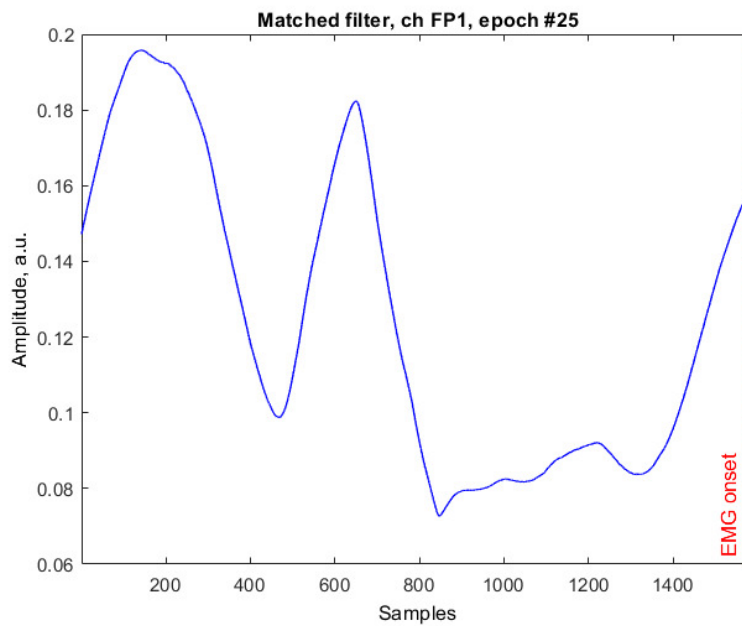


Figure 8.21: Detail of epoch 25, channel FP1, subject 1. No significant peaks occur in a time-window of 2 s prior to EMG onset.

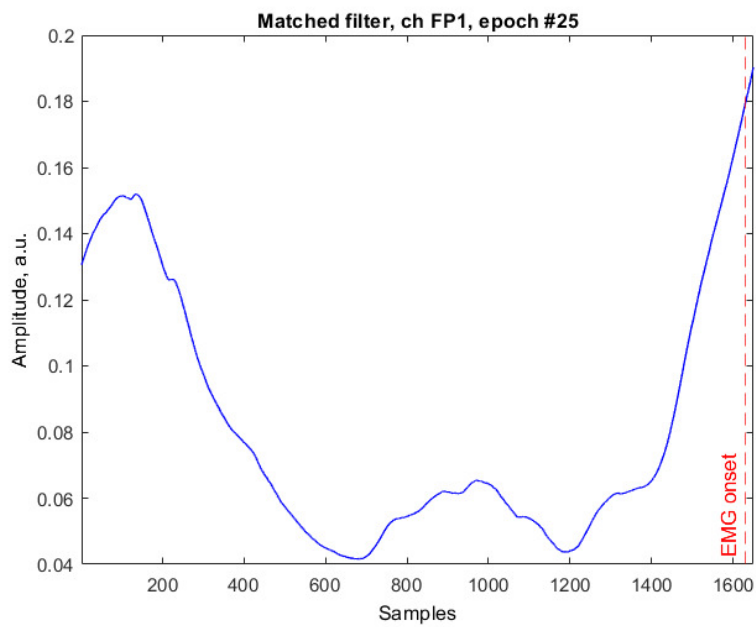


Figure 8.22: Detail of epoch 32, channel FP1, subject 1. No significant peaks occur in a time-window of 2 s prior to EMG onset.

## 8.6 Data interpretation

Different statistical considerations are made for the first dataset and the other two, respectively. The following sections describe the results obtained by applying the methods introduced in section 7.8.

### 8.6.1 Dataset 1: results

The Pearson coefficient is computed for 6 random subjects in the conditions described in section 7.8, paragraph *First dataset*. The results are shown in table 8.3.

	FC3-FCz	FC4-FCz	C3-Cz	C4-Cz	FC3-FC4	C3-C4
<b>Sub 1</b>	0.2	-0.12	0.27	0.45	-0.76	0.78
<b>Sub2</b>	0.95	0.89	-0.14	0.69	0.81	-0.8
<b>Sub 3</b>	0.89	0.53	0.88	0.65	0.37	0.6
<b>Sub 4</b>	0.98	0.86	0.94	0.08	0.87	0.37
<b>Sub 5</b>	0.95	0.5	0.92	0.62	0.37	0.82
<b>Sub 6</b>	0.85	-0.43	0.95	0.89	-0.13	0.95

Table 8.3: Pearson coefficient. Dataset 1, voluntary task.

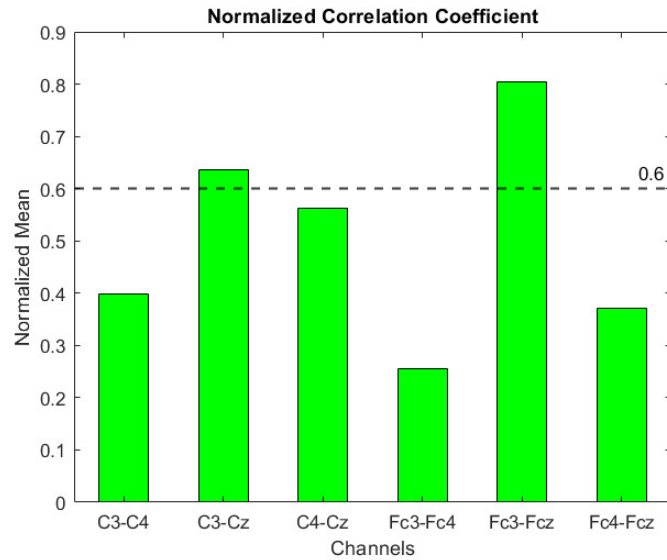


Figure 8.23: Mean correlation coefficient.

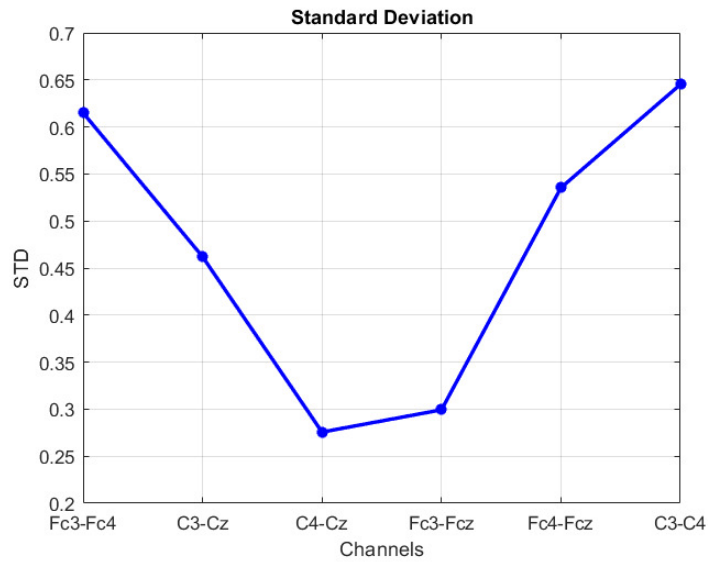


Figure 8.24: Standard deviation of the calculated correlation coefficient.

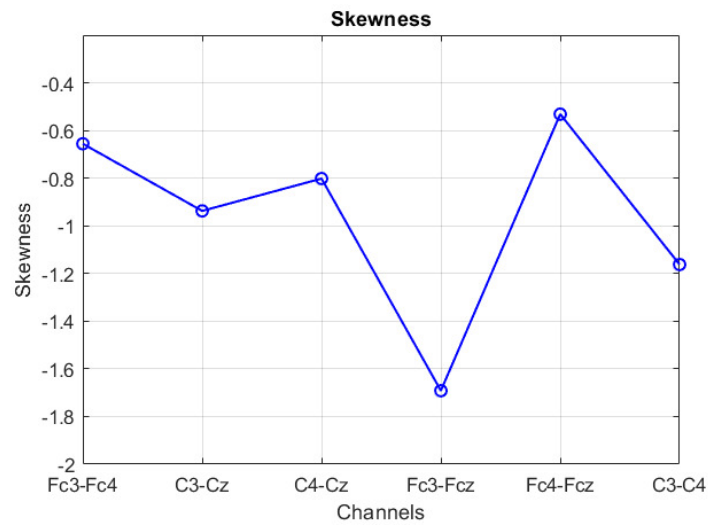


Figure 8.25: Skewness of the calculated correlation coefficient.

Figure 8.23 shows the mean correlation coefficient in the six conditions; the correlation threshold was set to 0.6. It is observed that left-positioned channels have higher correlation with the central reference with respect to right-position channels, suggesting that the potential is lateralized and generating on the left half of the cerebrum – as expected, since the movements were performed with the right hand. Moreover, contralateral channels prove to have little correlation (below 0.4). Figure 8.24 shows the standard deviation of the Pearson coefficient for the six considered

conditions. Focusing on C3–Cz, FC3–FCz comparison, it is possible to observe that the two have relatively small standard deviation – 0.46 and 0.3 respectively. Moreover, data feature negative skewness, meaning their distribution is leaning to the right (Figure 8.25).

### 8.6.2 Datasets 2 and 3: results

In this case, the aim was to investigate the similarity between the cortical potentials of the voluntary task and those of the semivoluntary task. The Pearson coefficient is calculated, for each channel, between MRCPs related to the two conditions above. The mean over all subjects is shown in Figure 8.26. The correlation threshold is set at a value of 0.5 – although values of 0.4 or higher are already considered acceptable. Electrodes positioned over the occipital lobe (O) feature low correlation, as expected: they record activity related primarily to visual and somatosensory information processing; the same holds for the electrodes allocated in the parietal and prefrontal cortex (P, FP). Higher correlation is found in PMC channels (C, FC, F); the result suggests that the functional area is the main source of cortical potentials, regardless of the nature of the performed task.

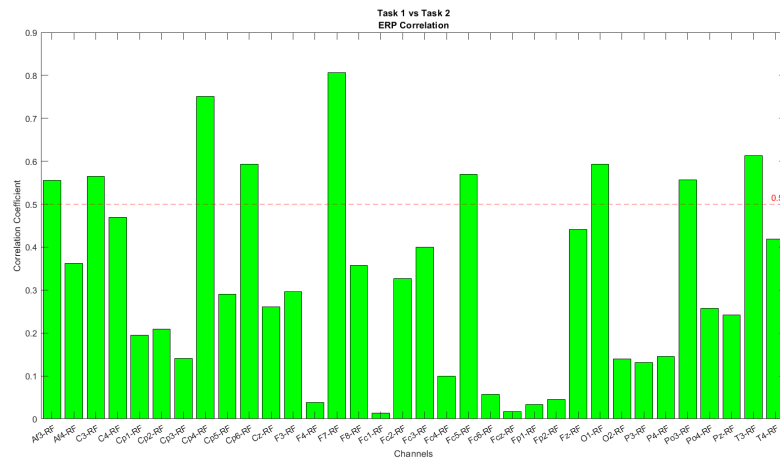


Figure 8.26: Pearson coefficient for task comparison; the correlation threshold is set at 0.5

# Chapter 9

## Future development: a Machine Learning approach

In section 7.8, the aim was to investigate the differences and similarities of cortical potentials elicited in different tasks. The last part of this work focused on the implementation of a machine learning algorithm that could discriminate between two essential tasks: voluntary and semivoluntary. The chosen classifier is *Support Vector Machine*.

### 9.1 Support Vector Machine

A Support Vector Machine (SVM) is a discriminative classifier, defined by a separating hyperplane. SVMs are *supervised learning* models that help classify data according to specific criteria. Given a *training set*, containing labelled data according to the output classes needed, a SVM classifier is able to assign new data to the correct category. This is performed by finding the hyperplane that best fits the examples provided. In two-dimensional space, the hyperplane is, in fact, a line that divides a plane in two parts where each part represents a class; it is easy to find the hyperplane that correctly separates the two categories (Figure 9.1). Given a training set made of  $n$  points such that:

$$(\vec{x}_1, y_1), \dots, (\vec{x}_n, y_n) \quad (9.1)$$

Where  $y_i$  indicates the class to which the element  $x_i$  belongs; the aim is to find the hyperplane that maximizes the margin between the points belonging to the different classes. The hyperplane is defined as follows:

$$\vec{w} \cdot \vec{x} - b = 0 \quad (9.2)$$

Another important parameter is  $\gamma$ , that defines the extent to which a single element in the training set influences the classification. Low  $\gamma$  results in the fact that also

data far from the hyperplane contributes to classification, high  $\gamma$  values indicate that only data found close to the hyperplane is considered in the calculation.

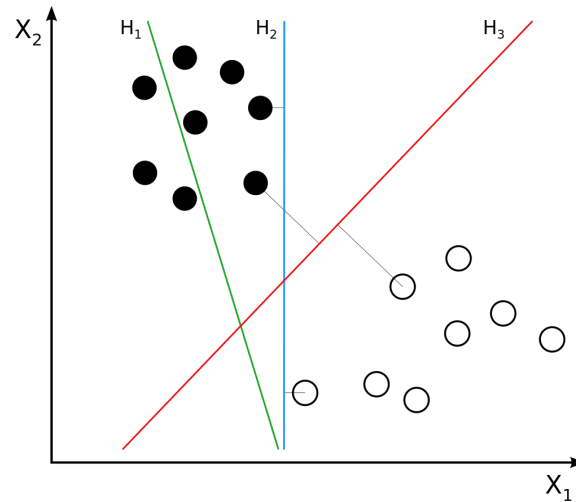


Figure 9.1: Two different sets of data and three hyperplanes;  $H_1$  is not able to separate data,  $H_2$  does but the margin is small and  $H_3$  separates them with maximum margin.

## 9.2 Implementation

As mentioned in the introduction, the SVM model was implemented in order to be able to classify the MRCPs in two classes: voluntary and semivoluntary. To this purpose, the training set consisted of a 68-rows matrix, corresponding to the observations – MRCP channel data. The model consisted of a 5-fold cross-validation – aiming at removing redundant variables and reducing overfitting, 5 predictors and 2 classes. The predictors were:

1. **Mean value;**
2. **Standard deviation;**
3. **Maximum value;**
4. **Minimum value;**
5. **Skewness.**

The two classes were indicated as follows:

1. **Voluntary:** label '1';

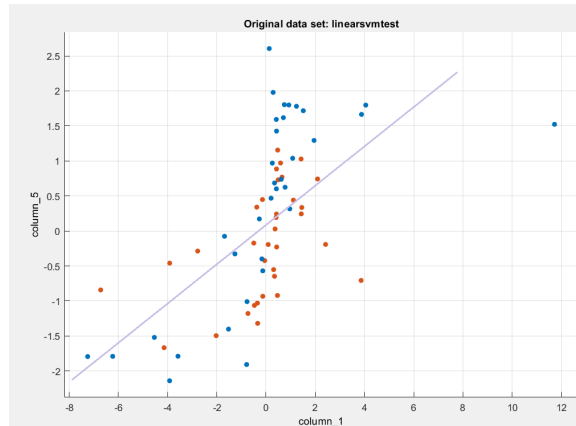


Figure 9.2: Scatter plot of the implemented model, the two classes are represented in orange (voluntary) and blue (semivoluntary). The purple line represents the separating hyperplane.

2. **Semivoluntary:** label '-1'.

The experimental data constituting the training set were not completely linearly separable and overlapped at some point in the scatter plot (Figure 9.2). However, it was possible to implement the linear classifier using a linear kernel function.

## 9.3 Results

The chosen model proved to be quite successful. The obtained values are the following:

- **Accuracy:** 63.2%;
- **Sensitivity:** 56%;
- **Specificity:** 29%;
- **Area Under the Curve:** 0.71.

The **Confusion Matrix** and **ROC** curve are shown in Figure 9.3, 9.4. The **Area Under the Curve** is 0.71, meaning that the implemented classifier is moderately accurate.



Figure 9.3: Confusion Matrix obtained as output from the implemented linear classifier.

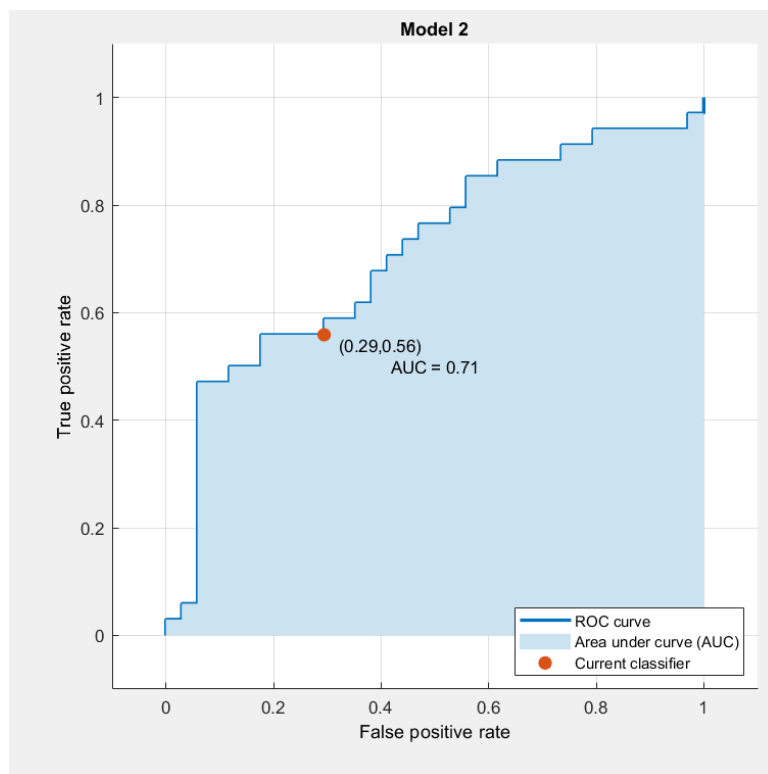


Figure 9.4: ROC curve from the implemented linear classifier.

# Conclusions

The experimental work presented in this Master Thesis consisted in a combination of Biomedical Engineering and Computational Neuroscience techniques. I had the possibility to work on something that I am passionate about, to apply the skills acquired during Bachelor and Master education and, most importantly, to learn. The human brain is a very complex machine; the aim of this study was to identify the differences between voluntary and involuntary patterns elicited by the cerebral cortex and find evidence of the effect of habit during task performing. By applying the methods described in Chapter 7, it was possible to demonstrate the uprising of the intention of performing actions in healthy adult subjects. This is represented by the presence of the Motor Related Cortical Potentials, that occur about 2 s before the movement is actualized, and whose most investigated component is the Readiness Potential. This factor is said to be lateralized; in fact, the cortical potentials can be observed all over the scalp, but they generate contralaterally with respect to the side of the body that is controlled. The MRCPs extracted from Single Trial EEG data were used to prove this assumption; by using the electrodes positioned over the longitudinal fissure as reference, the cross-correlation coefficient was computed and Pearson coefficient values higher than **0.6** were found between the contralateral electrodes and the reference. Furthermore, it was possible to locate the MRCPs in the EEG frequency spectrum; although electroencephalographic activity of the subjects undergoing the tasks was located in the  $\beta$  - *band*, the cortical potentials feature low and very low frequency components, positioning themselves in the frequency spectrum below **7 Hz**. After demonstrating the nature of the Motor Related Cortical Potentials, they were used in a convolution operation with Single Trial EEG data recorded during the performance of a semivoluntary task, in order to prove the effect of habit on brain electrical activity. The output of the implemented matched filter proved that during the first part of the trial, the brain still responded as it was planning and actualizing a volitional movement; nevertheless, it is shown that towards the end of the trial there is no significant matching of the EEG data. This proves that cortical activity undergoes adjustment during repetitive task execution. Afterwards, it was demonstrated, through the computation of the Pearson coefficient, that voluntary and semivoluntary tasks, respectively, generate MRCPs that are different but not entirely uncorrelated. In fact, values of Pearson

coefficient larger than **0.5** could be found in the channels covering the primary motor cortex; this suggests that the activation pattern is similar. Lastly, proved that there is difference in cerebral cortical activations during the two different tasks, in the view of future development, a Machine Learning approach was followed, aiming at discriminating between the two tasks. By applying the technique described in Chapter 9, a Support Vector Machine linear model was implemented and resulted in 63.2% accuracy, with true positive rate of 56%. This suggests that voluntary and semivoluntary patterns can be recognised and classified by implementing Machine Learning algorithms based on features such as amplitude and first and second order statistics parameters.

# List of Acronyms

**ABI** Acquired Brain Injury

**ANS** Autonomic Nervous System

**BCI** Brain Computer Interface

**BP** Bereitschaftspotential

**CBF** Cerebral Blood Flow

**CLIS** Complete Locked-In Syndrome

**CMRR** Common Mode Rejection Ratio

**CNS** Central Nervous System

**CNV** Contingent Negative Variation

**CSD** Current Scalp Density *or* Current Source Density

**CSF** Cerebrospinal Fluid

**DAQ** Data Acquisition

**DBS** Deep Brain Stimulation

**ECG** Electrocardiography

**ECoG** Electrocorticography

**EEG** Electroencephalography

**EMG** Electromyography

**ERP** Event-Related Potentials

**FIR** Finite Impulse Response

**fMRI** Functional Magnetic Resonance Imaging

<b>GCS</b>	Glasgow Coma Scale
<b>GUI</b>	Graphical User Interface
<b>HF</b>	High Frequency
<b>ICA</b>	Independent Component Analysis
<b>LF</b>	Low Frequency
<b>LIS</b>	Locked-In Syndrome
<b>LRP</b>	Lateralized Readiness Potential
<b>MA</b>	Moving Average
<b>MCS</b>	Minimally Conscious State
<b>MEG</b>	Magnetoencephalography
<b>MLF</b>	Medium-Low Frequency
<b>MP</b>	Motor Potential
<b>MRCP</b>	Motor Related Cortical Potential
<b>NS</b>	Negative Slope
<b>PET</b>	Positron Emission Tomography
<b>PMC</b>	Primary Motor Cortex
<b>PMP</b>	Pre Motion Positivity
<b>PSD</b>	Power Spectral Density
<b>PVS</b>	Persistent Vegetative State
<b>ROC</b>	Receiver Operating Characteristics
<b>SMA</b>	Supplementary Motor Area
<b>SRT</b>	Standard Reaction Time
<b>SSIF</b>	Spherical Spline Integral Filter
<b>SVM</b>	Support Vector Machine
<b>TBI</b>	Traumatic Brain Injury

*List of Acronyms*

---

**TKEO** Teager-Kaiser Energy Operator

**UCSF** University of California, San Francisco

**VLF** Very Low Frequency

# Bibliography

- [1] 13.2 the central nervous system.
- [2] Eeg caps.
- [3] Introduction to cortical neurons.
- [4] The libet experiment.
- [5] Lobes of the brain.
- [6] Mizar sirius system.
- [7] New method allows the study and identification of proteins in brain cellcell interactions.
- [8] JAV Bates. Electrical activity of the cortex accompanying movement. *The Journal of physiology*, 113(2-3):240–257, 1951.
- [9] R Benecke, JPR Dick, JC Rothwell, BL Day, and CD Marsden. Increase of the Bereitschaftspotential in simultaneous and sequential movements. *Neuroscience letters*, 62(3):347–352, 1985.
- [10] Christiaan Burger and David Jacobus van den Heever. Removal of eeg artefacts by combining wavelet neural network and independent component analysis. *Biomedical Signal Processing and Control*, 15:67–79, 2015.
- [11] De Rossi Carpi. Potenziali elettroencefalografici e potenziali evocati.
- [12] Thierry Castermans, Matthieu Duvinage, Guy Cheron, and Thierry Dutoit. Towards effective non-invasive brain-computer interfaces dedicated to gait rehabilitation systems. *Brain sciences*, 4(1):1–48, 2014.
- [13] Ujwal Chaudhary, Niels Birbaumer, and Ander Ramos-Murguialday. Brain-computer interfaces for communication and rehabilitation. *Nature Reviews Neurology*, 12(9):513, 2016.
- [14] Mike X. Cohen. *Analyzing Neural Time Series Data*. The MIT Press.
- [15] Lüder Deecke, Peter Scheid, and Hans H Kornhuber. Distribution of readiness potential, pre-motion positivity, and motor potential of the human cerebral cortex preceding voluntary finger movements. *Experimental brain research*, 7(2):158–168, 1969.
- [16] Stéphanie Devuyst, Thierry Dutoit, Patricia Stenuit, Myriam Kerkhofs, and Etienne Stanus. Removal of eeg artifacts from eeg using a modified independent component analysis approach. In *2008 30th Annual International Conference of the IEEE Engineering in Medicine and Biology Society*, pages 5204–5207.

- IEEE, 2008.
- [17] P Dollfus, PL Milos, A Chapuis, P Real, M Orenstein, and JW Soutter. The locked-in syndrome: a review and presentation of two chronic cases. *Spinal Cord*, 28(1):5, 1990.
- [18] Antonino Greco, Nadia Mammone, Francesco Carlo Morabito, and Mario Versaci. Kurtosis, renyis entropy and independent component scalp maps for the automatic artifact rejection from eeg data. *International Journal of Signal Processing*, 2(4):240–244, 2006.
- [19] Giuseppina Inuso, Fabio La Foresta, Nadia Mammone, and Francesco Carlo Morabito. Brain activity investigation by eeg processing: wavelet analysis, kurtosis and renyi’s entropy for artifact detection. In *2007 International Conference on Information Acquisition*, pages 195–200. IEEE, 2007.
- [20] Md Kafiul Islam, Amir Rastegarnia, and Zhi Yang. Methods for artifact detection and removal from scalp eeg: A review. *Neurophysiologie Clinique/Clinical Neurophysiology*, 46(4-5):287–305, 2016.
- [21] Farshad Kheiri, Anatol Bragin, and Jerome Engel Jr. Functional connectivity between brain areas estimated by analysis of gamma waves. *Journal of neuroscience methods*, 214(2):184–191, 2013.
- [22] Jun-ichi Kitamura, Hiroshi Shibasaki, and Tohru Kondo. A cortical slow potential is larger before an isolated movement of a single finger than simultaneous movement of two fingers. *Electroencephalography and clinical Neurophysiology*, 86(4):252–258, 1993.
- [23] Jun-ichi Kitamura, Hiroshi Shibasaki, Akiteru Takagi, Hideo Nabeshima, and Akira Yamaguchi. Enhanced negative slope of cortical potentials before sequential as compared with simultaneous extensions of two fingers. *Electroencephalography and clinical neurophysiology*, 86(3):176–182, 1993.
- [24] Manousos A Klados, Christos L Papadelis, and Panagiotis D Bamidis. Regica: a new hybrid method for eeg artifact rejection. In *2009 9th International Conference on Information Technology and Applications in Biomedicine*, pages 1–4. IEEE, 2009.
- [25] Marco Knaflitz. *Bioingegneria elettronica e sicurezza*. Levrotto & Bella.
- [26] Hans Helmut Kornhuber and Lüder Deecke. Hirnpotentialänderungen beim menschen vor und nach willkurbewegungen dargestellt mit magnetbandspeicherung und ruckwärtsanalyse. In *Pflugers Archiv-European Journal of Physiology*, volume 281, page 52. SPRINGER VERLAG 175 FIFTH AVE, NEW YORK, NY 10010, 1964.
- [27] Xiaoyan Li, Ping Zhou, and Alexander S Aruin. Teager–kaiser energy operation of surface emg improves muscle activity onset detection. *Annals of biomedical engineering*, 35(9):1532–1538, 2007.
- [28] Hiroaki Masaki, Noriyoshi Takasawa, and Katuo Yamazaki. Enhanced negative slope of the readiness potential preceding a target force production task.

- Electroencephalography and Clinical Neurophysiology/Evoked Potentials Section*, 108(4):390–397, 1998.
- [29] Luca Mesin. *Introduction to Biomedical Signal Processing*. Il Mio Libro.
- [30] Chiara Moccia. Sviluppo di un metodo per l’acquisizione del segnale eeg e la rimozione degli artefatti in uno studio finalizzato all’individuazione dei readiness potentials. Master’s thesis, Politecnico di Torino, 2018.
- [31] Frank Netter. *Atlas of Human Anatomy*. Elsevier.
- [32] J Pernier, F Perrin, and O Bertrand. Scalp current density fields: concept and properties. *Electroencephalography and clinical neurophysiology*, 69(4):385–389, 1988.
- [33] François Perrin, J Pernier, O Bertrand, and JF Echallier. Spherical splines for scalp potential and current density mapping. *Electroencephalography and clinical neurophysiology*, 72(2):184–187, 1989.
- [34] G Pfurtscheller. Graphical display and statistical evaluation of event-related desynchronization (erd). *Electroencephalography and clinical neurophysiology*, 43(5):757–760, 1977.
- [35] Gert Pfurtscheller and A Aranibar. Event-related cortical desynchronization detected by power measurements of scalp eeg. *Electroencephalography and clinical neurophysiology*, 42(6):817–826, 1977.
- [36] Gert Pfurtscheller and A Aranibar. Evaluation of event-related desynchronization (erd) preceding and following voluntary self-paced movement. *Electroencephalography and clinical neurophysiology*, 46(2):138–146, 1979.
- [37] P Praamstra, DF Stegeman, MWIM Horstink, and AR Cools. Dipole source analysis suggests selective modulation of the supplementary motor area contribution to the readiness potential. *Electroencephalography and clinical neurophysiology*, 98(6):468–477, 1996.
- [38] Simone Rumac. Single-trial analysis of readiness potentials using empirical mode decomposition. Master’s thesis, Politecnico di Torino, 2018.
- [39] Hiroshi Shibasaki and Mark Hallett. What is the Bereitschaftspotential? *Clinical neurophysiology*, 117(11):2341–2356, 2006.
- [40] Hiroshi Shibasaki, Norihiro Sadato, Hugh Lyshkew, Yoshiharu Yonekura, Manabu Honda, Takashi Nagamine, Shugo Suwazono, Yasuhiro Magata, Akio Ikeda, Masahito Miyazaki, et al. Both primary motor cortex and supplementary motor area play an important role in complex finger movement. *Brain*, 116(6):1387–1398, 1993.
- [41] Semyon Slobounov, Mark Hallett, and Karl M Newell. Perceived effort in force production as reflected in motor-related cortical potentials. *Clinical neurophysiology*, 115(10):2391–2402, 2004.
- [42] Catherine Stamoulis and Bernard S Chang. Application of matched-filtering to extract eeg features and decouple signal contributions from multiple seizure foci in brain malformations. In *2009 4th International IEEE/EMBS Conference on*

- Neural Engineering*, pages 514–517. IEEE, 2009.
- [43] Cyndy Stanfield. *Fisiologia*. EdiSES.
  - [44] Shravani Sur and VK Sinha. Event-related potential: An overview. *Industrial psychiatry journal*, 18(1):70, 2009.
  - [45] Yi-Yuan Tang, Rongxiang Tang, Mary K Rothbart, and Michael I Posner. Frontal theta activity and white matter plasticity following mindfulness meditation. *Current opinion in psychology*, 2019.
  - [46] Marcello Tononi, Giulio; Massimini. *Nulla di pi grande*. Baldini & Castoldi.
  - [47] Irene Vigue. Bci based on movement related cortical potentials (mrtps).
  - [48] Wikipedia. Event-related potential — wikipedia, the free encyclopedia, 2019. [Online; checked 17-may-2019].
  - [49] Wikipedia. Magnetoencephalography — wikipedia, the free encyclopedia, 2019. [Online; checked 10-april-2019].